

# Arteriosclerosis, Thrombosis, and Vascular Biology

JOURNAL OF THE AMERICAN HEART ASSOCIATION



## **Characterization of Ion Channels Involved in the Proliferative Response of Femoral Artery Smooth Muscle Cells**

Pilar Ciudad, Alejandro Moreno-Domínguez, Laura Novensá, Mercé Roqué, Leire Barquín, Magda Heras, M. Teresa Pérez-García and José R. López-López

*Arterioscler Thromb Vasc Biol* 2010, 30:1203-1211: originally published online  
March 18, 2010

doi: 10.1161/ATVBAHA.110.205187

Arteriosclerosis, Thrombosis, and Vascular Biology is published by the American Heart Association,  
7272 Greenville Avenue, Dallas, TX 75214

Copyright © 2010 American Heart Association. All rights reserved. Print ISSN: 1079-5642. Online  
ISSN: 1524-4636

The online version of this article, along with updated information and services, is  
located on the World Wide Web at:

<http://atvb.ahajournals.org/content/30/6/1203>

Data Supplement (unedited) at:

<http://atvb.ahajournals.org/content/suppl/2010/03/17/ATVBAHA.110.205187.DC1.html>

Subscriptions: Information about subscribing to Arteriosclerosis, Thrombosis, and Vascular  
Biology is online at

<http://atvb.ahajournals.org/subscriptions/>

Permissions: Permissions & Rights Desk, Lippincott Williams & Wilkins, a division of Wolters  
Kluwer Health, 351 West Camden Street, Baltimore, MD 21202-2436. Phone: 410-528-4050. Fax:  
410-528-8550. E-mail:

[journalpermissions@lww.com](mailto:journalpermissions@lww.com)

Reprints: Information about reprints can be found online at

<http://www.lww.com/reprints>

## Characterization of Ion Channels Involved in the Proliferative Response of Femoral Artery Smooth Muscle Cells

Pilar Ciudad, Alejandro Moreno-Domínguez, Laura Novensá, Mercé Roqué, Leire Barquín, Magda Heras, M. Teresa Pérez-García, José R. López-López

**Objective**—Vascular smooth muscle cells (VSMCs) contribute significantly to occlusive vascular diseases by virtue of their ability to switch to a noncontractile, migratory, and proliferating phenotype. Although the participation of ion channels in this phenotypic modulation (PM) has been described previously, changes in their expression are poorly defined because of their large molecular diversity. We obtained a global portrait of ion channel expression in contractile versus proliferating mouse femoral artery VSMCs, and explored the functional contribution to the PM of the most relevant changes that we observed.

**Methods and Results**—High-throughput real-time polymerase chain reaction of 87 ion channel genes was performed in 2 experimental paradigms: an in vivo model of endoluminal lesion and an in vitro model of cultured VSMCs obtained from explants. mRNA expression changes showed a good correlation between the 2 proliferative models, with only 2 genes, Kv1.3 and Kv $\beta$ 2, increasing their expression on proliferation. The functional characterization demonstrates that Kv1.3 currents increased in proliferating VSMC and that their selective blockade inhibits migration and proliferation.

**Conclusion**—These findings establish the involvement of Kv1.3 channels in the PM of VSMCs, providing a new therapeutic target for the treatment of intimal hyperplasia. (*Arterioscler Thromb Vasc Biol.* 2010;30:1203-1211.)

**Key Words:** gene expression ■ ion channels ■ restenosis ■ vascular biology ■ vascular muscle ■ Kv1.3 channels ■ vascular remodeling

Vascular smooth muscle cells (VSMCs) are differentiated cells that regulate vessel diameter and determine tissue perfusion. However, they can exhibit a variety of functionally dissimilar phenotypes. In response to local cues, VSMCs experience a phenotypic modulation (PM), with profound and reversible changes leading to proliferation, migration, and secretion of extracellular matrix components.<sup>1</sup> This plasticity is essential for injury repair, but it also contributes to the development and progression of vascular disease in response to abnormal environmental signals. It is becoming evident that contractile and proliferative phenotypes represent extreme cases of a spectrum of phenotypes that may coexist as the result of a developmentally regulated genetic program constantly modulated by environmental cues. This explains both a relatively stable expression of certain transcriptional programs in different VSMCs and a marked plasticity of these cells, including the ability to respond with different genetic

programs to readjust cellular activity to mechanical and hormonal factors.<sup>1-3</sup>

### See accompanying article on page 1073

The switch in ion transport mechanisms associated with PM is getting increasing amounts of attention. Coordinate changes in ion channels are an integral component of VSMC plasticity, as they can redirect biochemical activity toward new functional responses.<sup>4,5</sup> Moreover, both contractile and proliferative signals require specific changes in intracellular [Ca<sup>2+</sup>] and membrane potential that are determined by the ion channels expressed in VSMCs. Remodeling of several ion channels has shown to be functionally important for the PM of VSMCs in several preparations.<sup>5-10</sup> These data contribute to our understanding of VSMC modulation, but also, importantly, they can provide new targets for the treatment of vascular disorders. To date, studies of ion channel distribution within specific vascular beds and the modifications of ion channels on

Received on: April 3, 2009; final version accepted on: March 10, 2010.

From Departamento de Bioquímica y Biología Molecular y Fisiología e Instituto de Biología y Genética Molecular, Universidad de Valladolid y Consejo superior de Investigaciones Científicas, Valladolid, Spain (P.C., A.M.-D., M.T.P.-G., J.R.L.-L.); Servicio de Cardiología. Institut Clinic del Tòrax, Hospital Clinic, Instituto de Investigaciones Biomedicales August Pi i Sunyer, Universidad de Barcelona, Barcelona, Spain (L.N., M.R., L.B., M.H.).

Correspondence to José Ramón López-López, Departamento de Bioquímica y Biología Molecular, Universidad de Valladolid, Edificio Instituto de Biología y Genética Molecular, c/ Sanz y Forés s/n, 47003 Valladolid, Spain. E-mail jrlopez@ibgm.uva.es

© 2010 American Heart Association, Inc.

*Arterioscler Thromb Vasc Biol* is available at <http://atvb.ahajournals.org>

DOI: 10.1161/ATVBAHA.110.205187

remodeling have been limited to a small number of candidate subunits believed to be of importance. In addition, the complexity of their characterization in the *in vivo* models has led most investigators to extrapolate from the data obtained from cultured VSMCs as a proliferative phenotype, because VSMCs in intimal hyperplastic lesions resemble dedifferentiated myofibroblasts or cultured VSMCs. However, the emerging picture regarding the phenotypic regulation of VSMCs shows a large degree of diversity, reflecting both intrinsic variability of VSMCs among vascular beds and the specific responses to the different proliferative signals present in cultured cells and in the *in vivo* lesions.

Here, we used a quantitative approach to obtain a global portrait of ion channel gene expression in contractile VSMCs from mouse femoral arteries and their changes on PM in 2 proliferative models: an *in vivo* model of neointimal hyperplasia induced by endoluminal lesion<sup>11</sup> and an *in vitro* model using cultured VSMCs from arterial explants. Two genes (Kv1.3 and Kv $\beta$ 2) showed a concordant upregulation in both models, and the expression and function of Kv1.3 proteins was explored. Electrophysiological studies in cultured VSMCs and VSMCs from injured arteries show an increased functional expression of Kv1.3 currents. Pharmacological or genetic Kv1.3 blockade inhibits cultured VSMC migration and proliferation, and this inhibition cannot be mimicked by VSMC depolarization. Finally, the analysis of other vascular beds confirms that upregulation of Kv1.3 associates with PM, suggesting that they can represent a good therapeutic target by which to control VSMC proliferation.

## Materials and Methods

An expanded Materials and Methods section is given in the supplemental material, available online at <http://atvb.ahajournals.org>.

### Animals

Blood pressure normal (BPN) mice (The Jackson Laboratory) were maintained with inbred crossing in the animal facilities of the schools of medicine of the universities of Valladolid and Barcelona. Unilateral transluminal injury of femoral arteries was performed by passage of a 0.25-mm-diameter angioplasty guide wire, as previously described.<sup>11</sup>

### VSMC Isolation

Mice were killed by decapitation after isoflurane anesthesia. Femoral arteries were dissected and cleaned of connective and endothelial tissues, and they were stored for RNA extraction or used directly to obtain fresh dispersed VSMCs or cultured VSMCs as previously described.<sup>8,12</sup>

### RNA Expression Profile

TaqMan low-density arrays (Applied Biosystems) were used to simultaneously quantify the expression of 96 genes per sample.<sup>12</sup> Each sample derived from  $\approx$ 500 ng of mRNA from contractile or proliferating VSMCs.

### Protein Expression and Function

Selective antibodies were used for protein detection with immunologic methods.<sup>8,11</sup> The whole-cell and perforated-patch configura-

tions of the patch-clamp technique were used for functional studies in isolated VSMCs.<sup>8,12</sup>

### Migration and Proliferation Studies

Migration of cultured VSMCs was studied by a scratch assay and proliferation was determined by 5-bromo-2'-deoxyuridine (BrdU) incorporation.

## Results

### Expression Profile of Ion Channel Genes in Femoral VSMCs

The transcriptional expression levels of 87 ion channel subunits in VSMCs from mouse femoral arteries were investigated by real-time polymerase chain reaction. These channel genes include  $\alpha$ ,  $\beta$ , and  $\gamma$  subunits of K<sup>+</sup> channels and  $\alpha$  subunits of voltage-dependent Ca<sup>2+</sup> channels, Cl<sup>-</sup> channels, and Trp channels. The expression levels of markers of VSMCs (calponin, Cnn1) and endothelium (endothelial nitric oxide synthase, Nos3, and von Willebrand factor), were also explored, as well as other endogenous controls (Gapdh, B2m, Hprt-1, and Klf5). Expression of 26 channel genes was undetectable after 40 cycles of amplification under all conditions.

The relative abundance of the 54 channel genes found in the control preparation (mRNA from intact femoral arteries, with endothelium, C<sub>E+</sub>) is shown in Figure 1. Genes are grouped by families, and their expression levels are normalized to the endogenous control ribosomal protein 18S. We detected expression of 1 Cl<sup>-</sup> channel (Clcn3) and several inward rectifier and 2-pore domain K<sup>+</sup> channels. We found expression of all members of the Ca<sup>2+</sup>-dependent K<sup>+</sup> channels (K<sub>Ca</sub>) family, with the exception of the maxiK (BK<sub>Ca</sub>)  $\beta$  subunit BK $\beta$ 2; of them, the BK $\alpha$  and BK $\beta$ 1 subunits were among the most abundantly expressed channel genes. Within the voltage-dependent K<sup>+</sup> channels (Kv channels), we found expression of several accessory subunits, as well as pore-forming  $\alpha$  subunits of members of the Kv1 to Kv4 and Kv11 subfamilies. Voltage-dependent Ca<sup>2+</sup> channels are represented by Cav1 and Cav3 subfamily members. Finally, we detected expression of a large number of Trp channels of the Trpc, Trpv, Trpm, and Trpp subfamilies, with Trpp2 being the most abundant transcript.

Changes in the expression profile of ion channels induced by the switch to a proliferative phenotype were studied in VSMCs obtained from explants of endothelium-denuded femoral arteries and kept in culture (*in vitro* model) and in endoluminal lesion-induced intimal hyperplasia (*in vivo* model), in which expression changes were studied at 3 different times after lesion (48 hours, 1 week, and 4 weeks). Each model had its own control: endothelium-free arteries (C<sub>E-</sub>) for the *in vitro* model and endothelium intact arteries (C<sub>E+</sub>) for the *in vivo* model. Differences between these 2 controls are summarized in the inset in Figure 1, where genes whose expression was modified in the C<sub>E-</sub> samples (relative to C<sub>E+</sub>) are shown.

Changes in proliferation were analyzed by 2 methods. First, we studied, for each individual gene, the differences

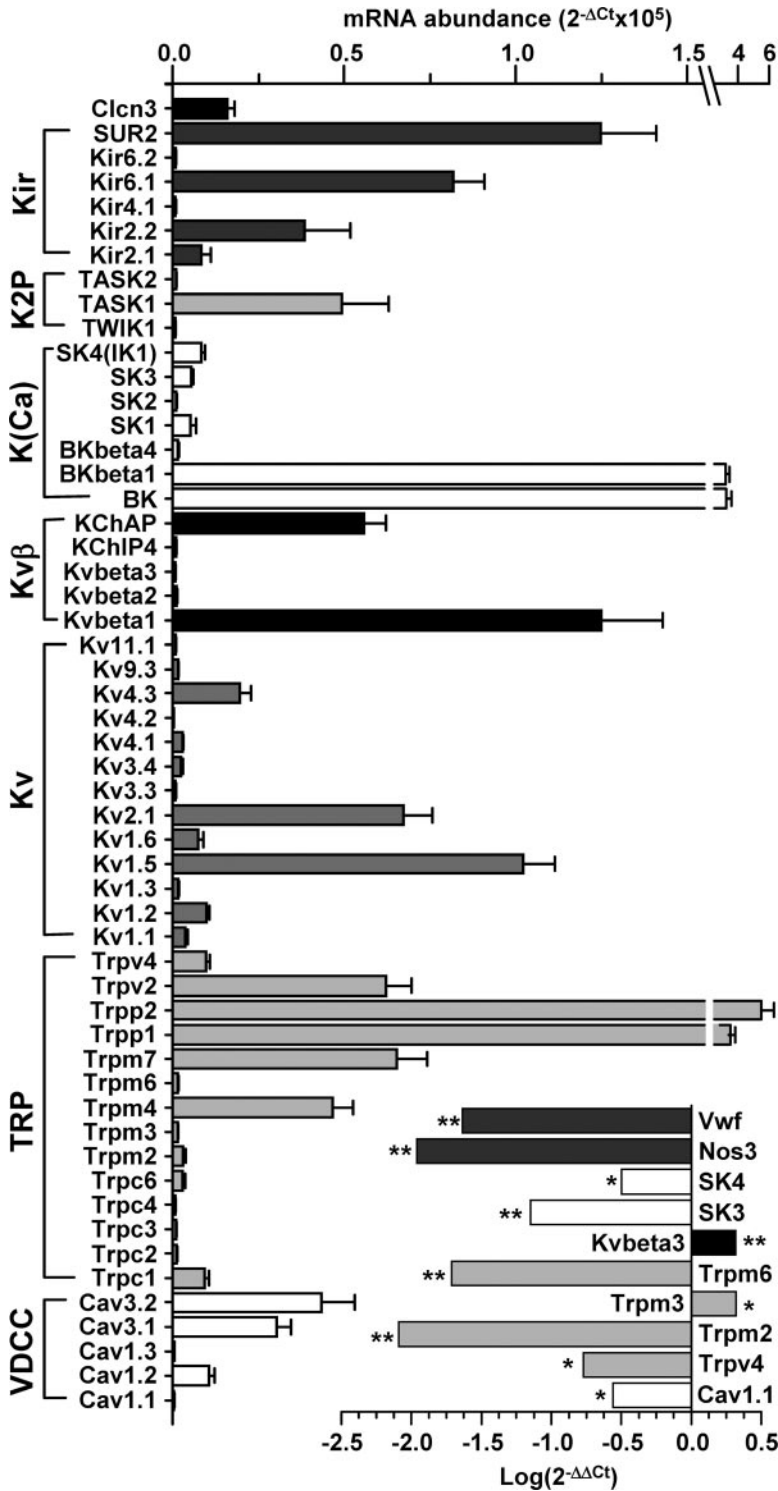


**Figure 1.** Relative abundance of the ion channel genes studied in complete femoral arteries ( $C_{E+}$ ) expressed as  $2^{-\Delta Ct}$ , where  $\Delta Ct = Ct_{channel} - Ct_{18s}$ . Each bar is the mean  $\pm$  SEM of 10 determinations obtained in 5 duplicate assays. Genes are grouped by families (see online supplemental data for the list of channel genes). The inset shows fold changes in expression in endothelium-free arteries ( $C_{E-}$ ) expressed as  $\text{log}(2^{-\Delta\Delta Ct})$ , where  $\Delta\Delta Ct = \Delta Ct(C_{E-}) - \Delta Ct(C_{E+})$ . In all figures, \* $P < 0.05$ , \*\* $P < 0.01$ , and \*\*\* $P < 0.001$ .

between control and proliferation in the 2 models by using the  $2^{-\Delta\Delta Ct}$  relative quantification method<sup>13</sup> (Supplemental Figure III). Second, a 2-way hierarchical clustering analysis of genes and different experimental conditions<sup>14</sup> was performed and visualized with the Treeview software (Figure 2). This analysis categorized genes according to their responses to PM into upregulated and downregulated genes and also demonstrated time-course-related subclass-

sifications in the model of endoluminal lesion (Figure 2A). Groups of genes with similarity in the pattern of expression (indicated by the correlation coefficient) are highlighted in Figure 2. Within downregulated genes, we identified clusters of genes with late decrease expression (Figure 2, box A), early decrease followed by a partial recovery (box B), or time-independent decrease (box C). Similarly, PM-upregulated genes can show a late increase

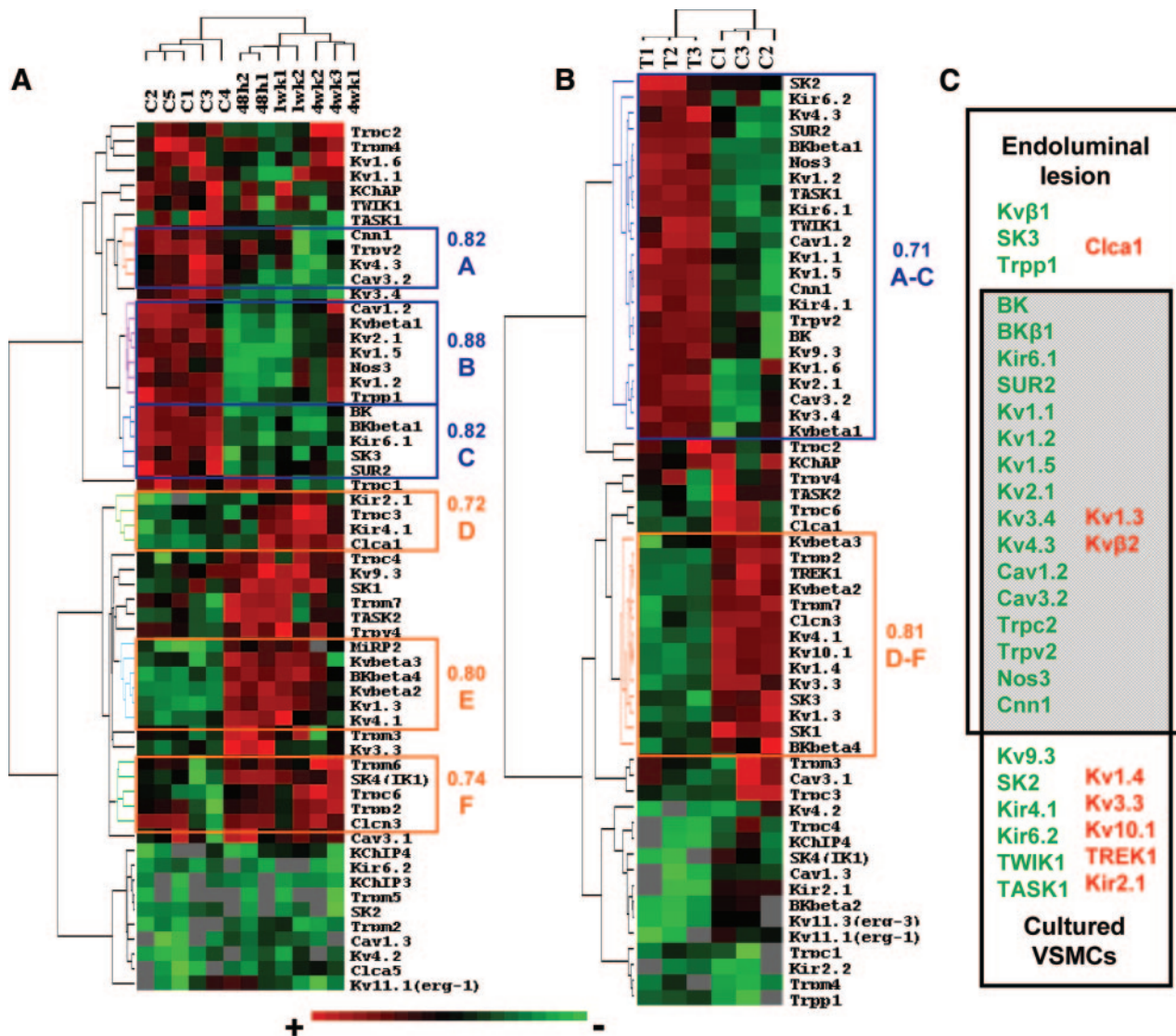


**Figure 2.** A, Two-way hierarchical agglomerative clustering applied to 59 genes (horizontally) and to 5 contractile VSMCs samples (C1 to C5), 2 samples at 48 hours after endoluminal lesion, 2 samples after 1 week, and 3 samples after 4 weeks (vertically). The input data were the  $\Delta Ct$  values for the genes. Color patch represents the expression level for each gene and sample. Expression levels were normalized within each sample, with a scale ranging from bright green (lowest) to bright red (highest). Missing values are shown as gray patches. The length of the tree branches is proportional to the correlation of the gene expression pattern, and some of these clusters and correlation coefficients are indicated. B, Same representation as in A, but comparing the contractile VSMCs (labeled here as tissues T1 to T3) with the cultured VSMCs (C1 to C3). C, Diagram showing genes exhibiting significant expression changes (upregulation, red font or downregulation, green font) in endoluminal lesion samples and in cultured VSMCs, when analyzed with the T-REX set of tools of the GEPAS suite (see Supplemental Methods). The light gray intersection contains the genes showing the same significant changes in both models.

(box D), an early increase with partial recovery (box E), or a sustained increase (box F). Following these criteria, the hierarchical clustering of the genes whose expression was modified in cultured VSMC (Figure 2B) also identified 2 groups of genes with decreased (boxes A through C) or increased (boxes D through F) expression with proliferation.

To discern whether these expression patterns were simply arbitrary structures or rather reflect biologically significant associations, we performed a statistical analysis of the data with the GEPAS suite (<http://gepas.bioinfo.cipf.es/>), with false discovery rate (FDR) correction.<sup>15</sup> We

obtained a significant variation in the expression of 22 genes in the in vivo model and 29 genes in the in vitro model (Figure 2C). The endoluminal lesion induced a significant increase in 3 genes (ClCa1, Kv1.3, and Kvβ2), and a significant decrease in 19 genes. In cultured VSMCs, 7 genes were overexpressed and 22 exhibited significant decrease. The overlapping region in Figure 2C shows the genes with significant changes in their expression profile common to both proliferative models (18 genes). Of them, we focused on those with increased expression (Kv1.3 and Kvβ2), as they are more amenable to represent therapeutic targets. We studied the presence, distribution, and

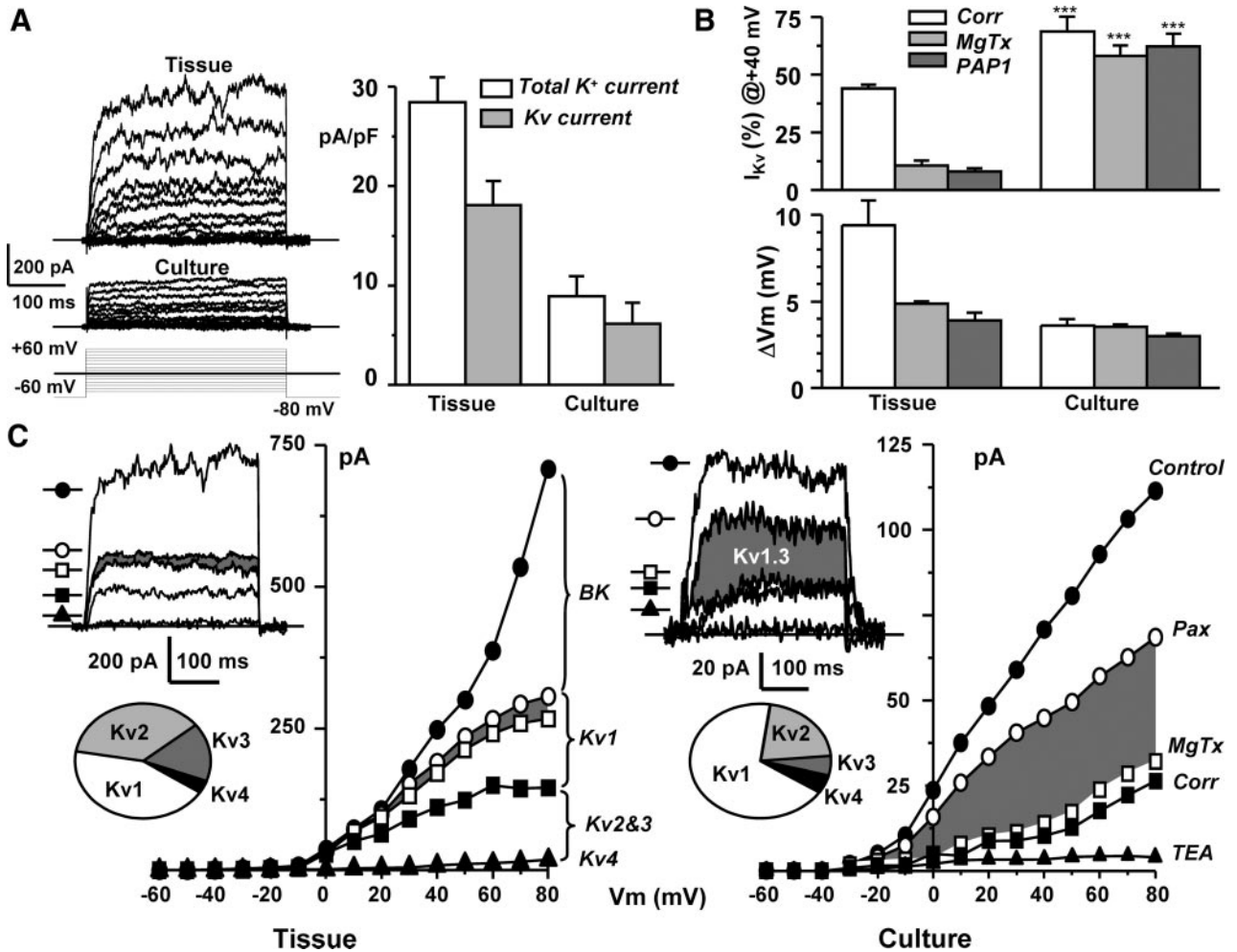


**Figure 3.** A, Family of current traces obtained in freshly dissociated and cultured VSMCs with the indicated pulse protocol. Current density of the total outward K<sup>+</sup> current was calculated in depolarizing pulses to +40 mV. Kv current density was obtained after BK<sub>Ca</sub> block with 500 nmol/L paxilline. Mean±SEM of 14 to 18 cells. B, The upper plot shows the fraction of the total Kv current represented by Kv1.x currents (correolide-sensitive) and Kv1.3 currents (margatoxin- or PAP1-sensitive) in contractile (tissue) versus cultured VSMCs. The amplitude of the depolarization induced by these blockers in perforated-patch recordings is represented in the lower plot. Mean±SEM of 11 to 14 cells. C, Pharmacological characterization of outward K<sup>+</sup> currents in contractile and cultured VSMCs. Shown are current/voltage relationships obtained in 2 cells in control conditions and after sequential application of paxilline (500 nmol/L), margatoxin (10 nmol/L), correolide (5 μmol/L), and TEA (20 mmol/L). The Kv1.3 component is represented by the shaded areas. The traces show current at +80 mV in both cells with each blocker, and pie charts represent the proportion of Kv1-Kv4 currents in both preparations.

functional contribution of Kv1.3 in both proliferative models.

**Functional Expression of Kv Channels in Femoral VSMCs**

Outward K<sup>+</sup> currents were studied with the whole-cell patch clamp technique in freshly dissociated VSMCs and in cultured VSMCs from femoral arteries. Figure 3A shows representative traces obtained in each condition. Both total outward K<sup>+</sup> current density, and the Kv component of this current (ie, the 500 nmol/L paxilline-resistant current<sup>16</sup>) was significantly larger at all voltages in VSMCs in the contractile phenotype, but there were no significant differences in the proportion of the two components. However, the Kv1 fraction of the current (the 5 μmol/L correolide-sensitive current) was significantly

larger in cultured VSMCs (from 44.12±1.6% in tissue to 68.69±6.5% in culture, Figure 3B). The increased functional contribution of Kv1.3 channels can account for this change, as revealed by selective Kv1.3 blockers (margatoxin and PAP-1<sup>17,18</sup>). Current sensitive to 10 nmol/L margatoxin represented 58.15±4.54% of the Kv current in cultured VSMCs versus 10.66±2.03% in freshly dispersed VSMCs. Similar results were obtained with 10 nmol/L PAP-1. The functional contribution of these channels to set resting V<sub>M</sub> was explored with the same blockers, providing parallel results (Figure 3B, bottom). Figure 3C depicts examples of the pharmacological dissection of the outward K<sup>+</sup> currents. In the presence of paxilline (500 nmol/L), application of margatoxin or PAP-1 (10 nmol/L each) allowed quantification of the Kv1.3 component. After Kv1.3 blockade, correolide (5 μmol/L) was used to selec-

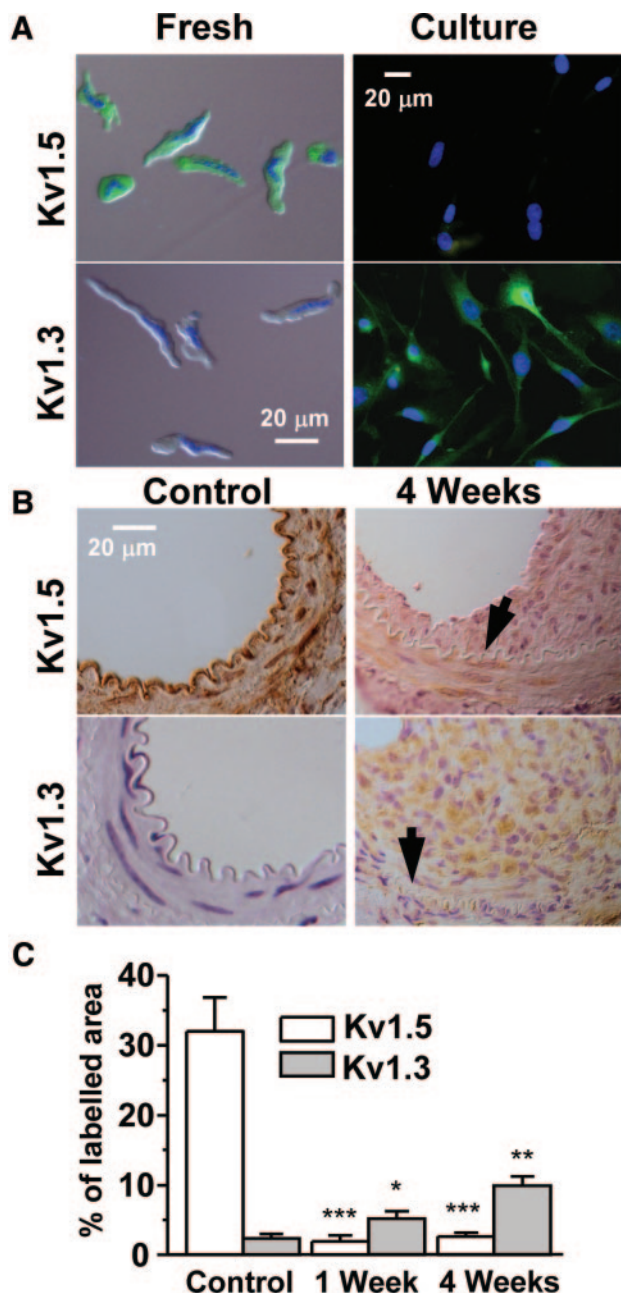


**Figure 4.** A, Immunocytochemical identification of Kv1.3 and Kv1.5 protein in freshly dispersed and cultured femoral VSMCs. Anti-Kv1.3 or anti-Kv1.5 labeling (green) is combined with 4',6-diamidino-2-phenylindole staining (blue) B, Paraffin sections of control and injured femoral arteries were labeled with the indicated antibodies and counterstained with hematoxylin. Arrows indicate internal elastic lamina (IEL). C, Summary data represent the percentage of labeled area over the total vessel area. Mean±SEM of 10 to 25 sections from 6 to 13 animals.

tively block the remaining Kv1 currents. Subsequent application of tetraethylammonium chloride (TEA) (20 mmol/L) identified the amplitude of the Kv2+Kv3 component. The minimal residual current, which was insensitive to correolide and TEA, could reflect Kv4 current component. The molecular composition of Kv currents in each preparation is illustrated in the pie charts.

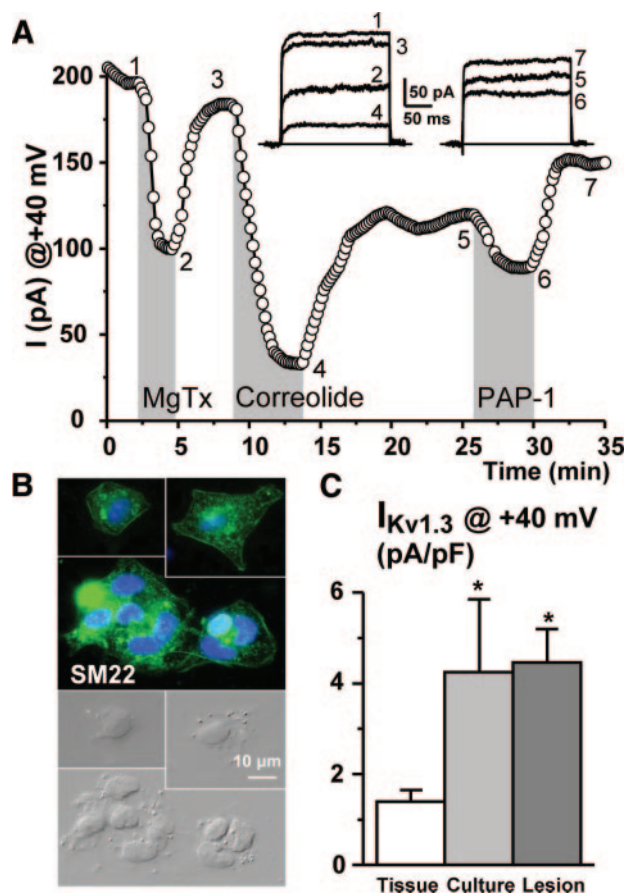


**Figure 5.** A, Representative example of the changes in peak current amplitude at +40 mV in a VSMC isolated from an injured artery with the indicated drugs. B, Labeling with anti-SM22 (green) demonstrates the vascular smooth muscle lineage of these cells. C, Absolute magnitude of the margatoxin-sensitive component ( $I_{Kv1.3}$ ) in control (contractile) and in cultured and injured VSMCs. Mean±SEM of 11 to 15 cells.

In addition to the increased proportion of Kv1 currents, cultured VSMCs also showed a significant decrease in the Kv2 (from  $36.52 \pm 2.97\%$  to  $21.34 \pm 3.71\%$ ) and Kv3 (from  $16.4 \pm 2.74\%$  to  $5.56 \pm 0.97\%$ ) components. The Kv3 component was estimated as the fraction of the currents blocked by 100  $\mu\text{mol/L}$  TEA after correolide, and the Kv2 component was calculated as the difference between 20 mmol/L and 100  $\mu\text{mol/L}$  TEA-sensitive currents.

### Kv1.3 Protein Expression in Femoral VSMCs

Changes in Kv1.3 protein expression were explored by immunocytochemistry in freshly dispersed and cultured VSMCs and by immunohistochemical labeling in sections of control and injured femoral arteries. We have also studied Kv1.5 protein expression as one example of channel downregulated on PM. Kv1.3 labeling increased in cultured VSMCs when compared with freshly dispersed cells, whereas Kv1.5 labeling disappeared (Figure 4A). Figure 4B shows similar results in sections of femoral arteries: Kv1.3 staining was weak in control sections, and increased after lesion (mainly in the intimal layer),

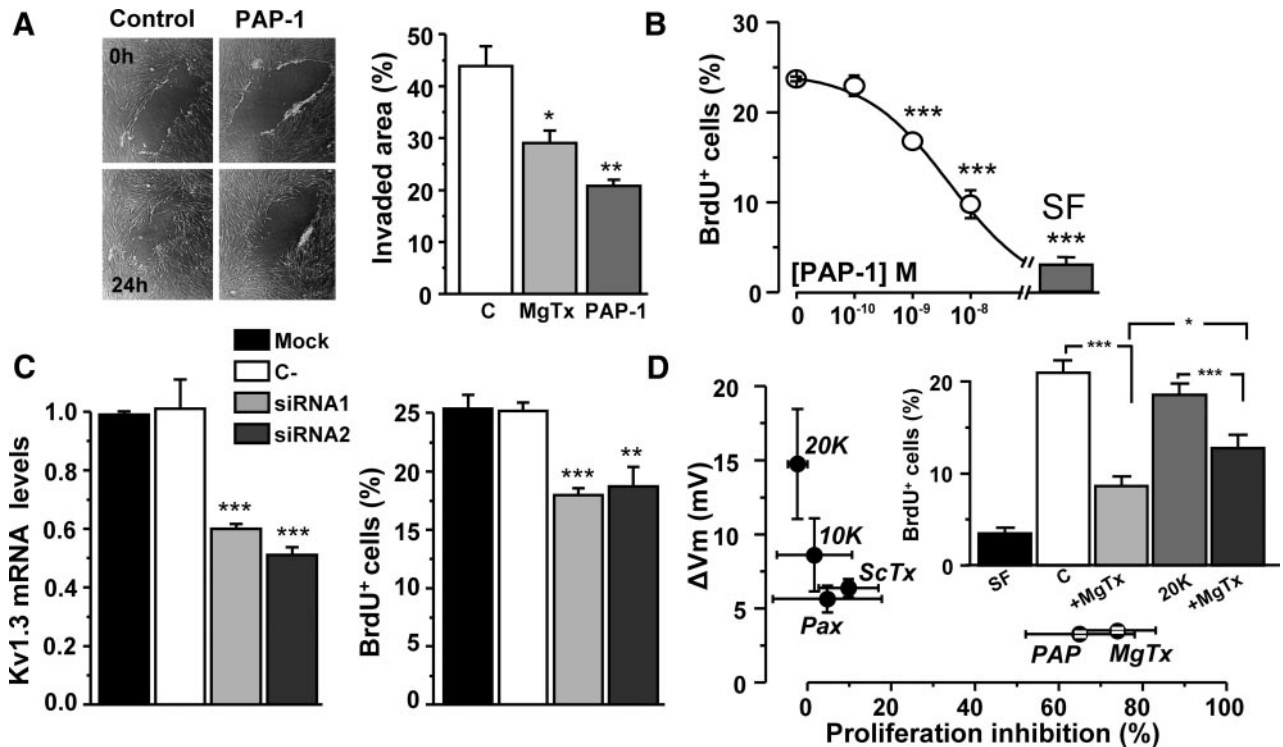


**Figure 6.** A, Effect of Kv1.3 blockers on femoral VSMC migration calculated as the percentage of invaded area in scratch assays. Images show a representative experiment with 10 nmol/L PAP-1. B, Dose-response effect of PAP-1 on the proliferation rate of cultured femoral VSMCs measured with a BrdU incorporation assay. n=3 to 8 experiments in each group; SF indicates serum-free medium. C, Two different Kv1.3 short interfering RNAs (siRNAs) were able to reduce mRNA expression (normalized to Gapdh) and BrdU incorporation in transfected VSMCs compared with mock-transfected or siRNA C - transfected VSMCs (n=4). D, Effects of K channel blockers or high [K<sup>+</sup>]<sub>e</sub> on resting V<sub>M</sub> (current-clamp experiments) and on proliferation inhibition (BrdUrd incorporation). Mean±SEM of 8 to 20 determinations. The inset shows the antiproliferative effect of MgTx (10 nmol/L) in control medium and in 20 mmol/L K<sup>+</sup>-containing medium. n=7 experiments.

whereas labeling with anti-Kv1.5 antibody was detected in the muscular layer of almost half of the cells in control arteries, decreasing on injury. Functional characterization of Kv1.3 currents from VSMCs obtained from injured arteries (Figure 5A) showed an augmented expression of the Kv1 component (85.2±4.5% of the Kv current) due to an increase of the MgTx-sensitive component (61.5±5.2%), very similar to the case with cultured VSMCs (see Figure 3B). Moreover, increased Kv1.3 current was not simply reflecting downregulation of other Kv channels, as Kv1.3 current density increased in both proliferation models (Figure 5C).

**Effects of Kv1.3 Blockade on VSMC Migration and Proliferation**

The upregulated functional expression of Kv1.3 could reflect a link between the channel and the establishment and maintenance of the proliferative phenotype. To explore this, we studied the effect of Kv1.3 current blockade on the ability of cultured VSMCs to migrate and proliferate. Migration was determined in confluent femoral VSMCs by a scratch migration assay. After 24 hours in serum-free medium alone (control) or with 10 nmol/L PAP-1 or 10 nmol/L margatoxin, the invaded area was significantly larger in control cells than in cells treated with the Kv1.3 blockers (Figure 6A). Similarly, the pro-

liferation rate, determined by the number of BrdU<sup>+</sup> cells, was significantly decreased by Kv1.3 channels blockade (Figure 6B through 6D). The effect of PAP-1 inhibiting proliferation was dose dependent (Figure 6B) and could be mimicked by selective knockdown of Kv1.3 currents with short interfering RNA (Figure 6C). PAP-1 and margatoxin depolarized VSMCs, but other maneuvers that also depolarized cultured VSMCs, such as increasing [K<sup>+</sup>]<sub>e</sub> or blockade of Kv2 or BK<sub>Ca</sub> channels, did not affect proliferation (Figure 6D). Moreover, proliferation inhibition by 10 nmol/L margatoxin was attenuated but still significant in the presence of 20 mmol/L K<sup>+</sup>e (Figure 6D, inset).

**Discussion**

This work provides a comprehensive study of the expression pattern of ion channels in VSMCs, using a quantitative high-throughput technique, with the goal of elucidating PM-associated changes. We defined the relative expression of the ion channel genes studied and compared this profile among different vascular beds, observing a continuous pattern that correlates with the size of the arteries (see Supplemental Figure IV), in agreement with previous data focused on individual channels.<sup>19-23</sup> Characterization of the changes in expression pattern associated with proliferation in in vivo and in vitro models of PM

showed a good correlation between both situations. Eighteen of 22 genes that changed in the *in vivo* model were conserved in cultured VSMCs. The larger number of genes that changed in cultured VSMCs can be attributed to their more homogeneous nature (a uniform population of synthetic VSMCs), whereas endoluminal lesion samples are partially contaminated with endothelial cells, contractile VSMCs, and connective tissue. These contaminants could also explain some of the changes present only in this model, as it is most likely the case of SK3 channels (small conductance  $K_{Ca}$  channels), whose expression is restricted to endothelial cells.<sup>9,24</sup> Although specific changes induced by the culture conditions cannot be excluded, our analysis indicates that ion channel expression profile in cultured VSMCs reproduces reasonably well the changes in proliferating lesions *in vivo*. This observation is important considering the technical limitations of the *in vivo* models for functional studies.

Only some of the channels highlighted here have been previously reported as relevant to VSMC proliferation. Downregulation of several Kv1 genes (Kv1.5, Kv1.2, and Kv2.1) has been reported in other preparations.<sup>8,25</sup> Also, decreased expression of Cav1.2 mRNA is consistent with the reported reduction in the functional expression of L-type  $Ca^{2+}$  channels in synthetic VSMCs,<sup>5,26</sup> although we did not detect the concomitant upregulation of genes of the Trpc and Cav3.x families described in these studies. Similarly, decreases of the BK channel genes (BK $\alpha$  and BK $\beta$ 1 subunits) have been described,<sup>5,8,9,27</sup> but we did not find the associated increase in IK1 mRNA that was previously reported.<sup>5,9,10</sup> Nevertheless, a contribution to PM in our preparation of these channels (Trpc, Cav3.x, or IK1) via posttranscriptional modulation cannot be excluded. Overall, vascular bed variations may account for some of the recounted discrepancies, and it is tempting to speculate that not only the expression profile of ion channels but also the PM-induced changes could be vascular bed specific. In this context, the finding of conserved changes across different preparations is relevant, as it may reflect obligatory associations of certain channels with vascular remodeling, representing novel therapeutic opportunities.

With this idea, we explored the functional expression and the contribution to VSMC proliferation of the genes upregulated by the PM. We focused on Kv1.3 channels because the tools for determining the contribution of the modulatory subunit Kv $\beta$ 2 are more limited. Furthermore, the concomitant increased expression of Kv1.3 and Kv $\beta$ 2 may reflect the fact that they form heteromultimers, because Kv $\beta$ 2 preferentially associates with Kv1.x channels,<sup>28</sup> and both association and upregulation of Kv1.3 and Kv $\beta$ 2 have been described on mitogen-stimulated activation of T lymphocytes.<sup>17,29</sup> Functional expression of Kv1.3 proteins increased in both proliferative models, and selective blockade of Kv1.3 currents decreased cultured VSMC migration and proliferation, demonstrating a link between Kv1.3 channels functional expression and PM. Finally, although Kv1.3 inhibition leads to VSMC depo-

larization, proliferation was not affected if depolarization was induced with other channel blockers or with high  $[K^+]_e$ .

However, Kv1.3 inhibition could restrain hyperpolarizing signals required for proliferation. This hypothesis is consistent with our results showing an attenuated response to MgTx in high  $[K^+]_e$ .

We have previously reported a similar association between Kv3.4 channel upregulation and proliferation in human uterine artery VSMCs,<sup>8</sup> although in this preparation, high  $[K^+]_e$  depolarization mimics proliferation inhibition by Kv3.4 blockade.<sup>30</sup> Interestingly, the Kv1.3 gene is also upregulated in these cells,<sup>8</sup> and Kv1.3 blockers inhibit proliferation (Supplemental Figure VIB and VIC), suggesting that the association between Kv1.3 upregulation and proliferation may be present in different vascular beds. In fact, the ion channel expression profile of cultured mesenteric VSMCs shows a remarkable similarity to that of femoral arteries (Supplemental Figure V), with Kv1.3 being the predominant Kv1 channel gene and Kv1.3 blockade inhibiting proliferation.

Kv1.3 channels have been reported to associate with proliferation in T cells,<sup>17</sup> endothelial cells,<sup>31</sup> microglia, macrophages, oligodendrocyte progenitors, and carcinoma cells,<sup>32,33</sup> but this is the first description of their role in VSMC proliferation and migration. In this scenario, Kv1.3 blockade could represent a new therapeutic approach to prevent unwanted remodeling.

### Acknowledgments

We thank Esperanza Alonso for excellent technical assistance and the Merck Company for the gift of corrololide.

### Sources of Funding

This work was supported by Ministerio de Sanidad, Instituto de Salud Carlos III grants R006/009 (Red Heracles), FS041139-0 (M.R.), and PI041044 (J.R.L.-L.); Ministerio de Educación y Ciencia grants BFU2004-05551 (M.T.P.-G.) and BFU2007-61524 (J.R.L.-L.); and Junta de Castilla y Leon grant GR242. Dr Moreno-Domínguez is a fellow of the Spanish Ministerio de Educación y Ciencia.

### Disclosures

None.

### References

- Owens GK, Kumar MS, Wamhoff BR. Molecular regulation of vascular smooth muscle cell differentiation in development and disease. *Physiol Rev*. 2004;84:767–801.
- Shanahan CM, Weissberg PL. Smooth muscle cell heterogeneity: patterns of gene expression in vascular smooth muscle cells *in vitro* and *in vivo*. *Arterioscler Thromb Vasc Biol*. 1998;18:333–338.
- Wamhoff BR, Bowles DK, Owens GK. Excitation-transcription coupling in arterial smooth muscle. *Circ Res*. 2006;98:868–878.
- Neylon CB. Potassium channels and vascular proliferation. *Vasc Pharmacol*. 2002;38:35–41.
- Beech DJ. Ion channel switching and activation in smooth-muscle cells of occlusive vascular diseases. *Biochem Soc Trans*. 2007;35:890–894.
- Gollasch M, Haase H, Ried C, Lindschau C, Morano I, Luft FC, Haller H. L-type calcium channel expression depends on the differentiated state of vascular smooth muscle cells. *FASEB J*. 1998;12:593–601.
- Kumar B, Dreja K, Shah SS, Cheong A, Xu SZ, Sukumar P, Naylor J, Forte A, Cipollaro M, McHugh D, Kingston PA, Heagerty AM, Munsch CM, Bergdahl A, Hultgardh-Nilsson A, Gomez MF, Porter KE, Hell-

- strand P, Beech DJ. Upregulated TRPC1 channel in vascular injury in vivo and its role in human neointimal hyperplasia. *Circ Res.* 2006;98:557–563.
8. Miguel-Velado E, Moreno-Dominguez A, Colinas O, Cidad P, Heras M, Perez-Garcia MT, López-López JR. Contribution of Kv channels to phenotypic remodeling of human uterine artery smooth muscle cells. *Circ Res.* 2005;97:1280–1287.
  9. Kohler R, Wulff H, Eichler I, Kneifel M, Neumann D, Knorr A, Grgic I, Kampf D, Si H, Wibawa J, Real R, Borner K, Brakemeier S, Orzechowski HD, Reusch HP, Paul M, Chandy KG, Hoyer J. Blockade of the intermediate-conductance calcium-activated potassium channel as a new therapeutic strategy for restenosis. *Circulation.* 2003;108:1119–1125.
  10. Tharp DL, Bowles DK. The intermediate-conductance Ca<sup>2+</sup>-activated K<sup>+</sup> channel (KCa3.1) in vascular disease. *Cardiovasc Hematol Agents Med Chem.* 2009;7:1–11.
  11. Roque M, Fallon JT, Badimon JJ, Zhang WX, Taubman MB, Reis ED. Mouse model of femoral artery denudation injury associated with the rapid accumulation of adhesion molecules on the luminal surface and recruitment of neutrophils. *Arterioscler Thromb Vasc Biol.* 2000;20:335–342.
  12. Moreno-Dominguez A, Cidad P, Miguel-Velado E, Lopez-Lopez JR, Perez-Garcia MT. De novo expression of Kv6.3 contributes to changes in vascular smooth muscle cell excitability in a hypertensive mice strain. *J Physiol.* 2009;587:625–640.
  13. Livak KJ, Schmittgen TD. Analysis of relative gene expression data using real-time quantitative PCR and the 2<sup>-ΔΔCt</sup> method. *Methods.* 2001;25:402–408.
  14. Eisen MB, Spellman PT, Brown PO, Botstein D. Cluster analysis and display of genome-wide expression patterns. *Proc Natl Acad Sci USA.* 1998;95:14863–14868.
  15. Gusnanto A, Calza S, Pawitan Y. Identification of differentially expressed genes and false discovery rate in microarray studies. *Curr Opin Lipidol.* 2007;18:187–193.
  16. Li G, Cheung DW. Effects of paxilline on K<sup>+</sup> channels in rat mesenteric arterial cells. *Eur J Pharmacol.* 1999;372:103–107.
  17. Beeton C, Wulff H, Standifer NE, Azam P, Mullen KM, Pennington MW, Kolski-Andreaco A, Wei E, Grino A, Counts DR, Wang PH, Lee-Healey CJ, Andrews S, Sankaranarayanan A, Homerick D, Roeck WW, Tehranzadeh J, Stanhope KL, Zimin P, Havel PJ, Griffey S, Knaus HG, Nepom GT, Gutman GA, Calabresi PA, Chandy KG. Kv1.3 channels are a therapeutic target for T cell-mediated autoimmune diseases. *Proc Natl Acad Sci USA.* 2006;103:17414–17419.
  18. Schmitz A, Sankaranarayanan A, Azam P, Schmidt-Lassen K, Homerick D, Hansel W, Wulff H. Design of PAP-1, a selective small molecule Kv1.3 blocker, for the suppression of effector memory T cells in autoimmune diseases. *Mol Pharmacol.* 2005;68:1254–1270.
  19. Jackson WF. Ion Channels and Vascular Tone. *Hypertension.* 2000;35:173.
  20. Michelakis ED, Reeve HL, Huang JM, Tolarova S, Nelson DP, Weir EK, Archer SL. Potassium channel diversity in vascular smooth muscle cells. *Can J Physiol Pharmacol.* 1997;75:889–897.
  21. Smith PD, Brett SE, Luykenaar KD, Sandow SL, Marrelli SP, Vigmond EJ, Welsh DG. KIR channels function as electrical amplifiers in rat vascular smooth muscle. *J Physiol.* 2008;586:1147–1160.
  22. Teramoto N. Physiological roles of ATP-sensitive K<sup>+</sup> channels in smooth muscle. *J Physiol.* 2006;572:617–624.
  23. Fountain SJ, Cheong A, Flemming R, Mair L, Sivaprasadarao A, Beech DJ. Functional up-regulation of KCNA gene family expression in murine mesenteric resistance artery smooth muscle. *J Physiol.* 2004;556:29–42.
  24. Jackson WF. Potassium channels in the peripheral microcirculation. *Microcirculation.* 2005;12:113–127.
  25. Mandegar M, Fung YC, Huang W, Remillard CV, Rubin LJ, Yuan JX. Cellular and molecular mechanisms of pulmonary vascular remodeling: role in the development of pulmonary hypertension. *Microvasc Res.* 2004;68:75–103.
  26. House SJ, Potier M, Bisailon J, Singer HA, Trebak M. The non-excitabile smooth muscle: calcium signaling and phenotypic switching during vascular disease. *Pflugers Arch.* 2008;456:769–785.
  27. Long X, Tharp DL, Georger MA, Slivano OJ, Lee MY, Wamhoff BR, Bowles DK, Miano JM. The smooth muscle cell-restricted KCNMB1 ion channel subunit is a direct transcriptional target of serum response factor and myocardin. *J Biol Chem.* 2009;284:33671–33682.
  28. Rhodes KJ, Strassle BW, Monaghan MM, Bekele-Arcuri Z, Matos MF, Trimmer JS. Association and colocalization of the Kvbeta1 and Kvbeta2 beta-subunits with Kv1 alpha-subunits in mammalian brain K<sup>+</sup> channel complexes. *J Neurosci.* 1997;17:8246–8258.
  29. McCormack T, McCormack K, Nadal MS, Vieira E, Ozaita A, Rudy B. The effects of shaker beta-subunits on the human lymphocyte K<sup>+</sup> channel Kv1.3. *J Biol Chem.* 1999;274:20123–20126.
  30. Miguel-Velado E, Perez-Carretero FD, Colinas O, Cidad P, Heras M, Lopez-Lopez JR, Perez-Garcia MT. Cell-cycle dependent expression of Kv3.4 channels modulates proliferation of human uterine artery smooth muscle cells. *Cardiovasc Res.* 2010;cvq011.
  31. Erdogan A, Schaefer CA, Schaefer M, Luedders DW, Stockhausen F, Abdallah Y, Schaefer C, Most AK, Tillmanns H, Piper HM, Kuhlmann CR. Margatoxin inhibits VEGF-induced hyperpolarization, proliferation and nitric oxide production of human endothelial cells. *J Vasc Res.* 2005;42:368–376.
  32. Pardo LA. Voltage-gated potassium channels in cell proliferation. *Physiology.* 2004;19:285–292.
  33. Wulff H, Castle NA, Pardo LA. Voltage-gated potassium channels as therapeutic targets. *Nat Rev Drug Discov.* 2009;8:982–1001.

# SUPPLEMENTAL MATERIAL

## MATERIAL AND METHODS

### *Animals and tissues*

BPN strain mice were purchased from Jackson Laboratories (Bar Harbor, Maine, USA) and maintained with inbred crossing in the animal facilities of the Schools of Medicine of Valladolid and Barcelona. Animals were housed under temperature-controlled conditions (21°C) with free access to water and food. Animal protocols were approved by the Institutional Care and Use Committee of the Universities of Valladolid and Barcelona, and are in accordance with the European Community guiding principles in the care and use of animals.

Uterine arteries were obtained from patients subjected to hysterectomy at the Clinic Hospital of Barcelona, with protocols approved by the Human Investigation Ethic Committee of the Hospital.

### *Surgical procedures and collection of arterial samples*

For the transluminal injury of femoral arteries, mice were anesthetized using isoflurane inhalation (5 % at 2.5 l O<sub>2</sub> min<sup>-1</sup>). Endoluminal lesion to the common femoral artery was achieved by 3 passages of a 0.25-mm-diameter angioplasty guidewire (Advanced Cardiovascular Systems) as previously described<sup>1</sup>. Briefly, a groin incision was made under a surgical microscope (Carl Zeiss), the femoral artery was temporarily clamped at the level of the inguinal ligament, and an arteriotomy was made distal to the epigastric branch. The guidewire was then inserted, the clamp removed, and the wire advanced to the level of the aortic bifurcation and pulled back. After removal of the wire, the arteriotomy site was ligated. Control sham-operated arteries underwent dissection, temporary clamping, arteriotomy, and ligature, without passage of the wire. The right femoral artery of mice underwent injury and the left artery was sham-operated and used as control.

To collect arterial samples mice were killed by decapitation after isoflurane anesthesia. VSMCs from femoral, mesenteric and aorta arteries were obtained after carefully dissection and cleaning of connective and endothelial tissues, and then arteries were either frozen at -80 °C to further extract RNA or used directly to obtain tissue explants or fresh dispersed VSMCs.

For the removal of endothelium, we explored the efficiency of chemical and mechanical methods by measuring the reduction in the expression of endothelial nitric oxide synthase (eNOS) using clean arteries with intact endothelium as the calibrator (see online supplemental figure I). In the light of these results, we combined detergent treatment (by perfusion of the arterial lumen during 10 min with a 0.1% Triton X-100 solution at a pressure of 80 mm Hg) followed by longitudinal section of the arteries and manual scrapping of the inner surface with a pipette tip to remove endothelium from the samples. Parallel measurements of calponin (Cnn1) mRNA levels were carried out in the same samples to ensure that the removal method did not produce changes in the smooth muscle layer.

At the indicated times after transluminal injury, femoral arteries were obtained from these mice as indicated above. However, the proliferative response after endoluminal lesion precluded the

identification and removal of endothelium in these samples, and consequently contralateral, sham-operated femoral arteries were also collected with intact endothelium to serve as controls. This control group was designated as CE+, while the endothelium-free arterial samples were labelled as CE-. The differences in the expression profile of the genes under study between these two conditions (CE+ and CE-) were also addressed (see below).

### ***VSMCs isolation***

For dispersed cells, small pieces of endothelium-free artery were placed in SMDS Ca<sup>2+</sup> free solution containing 0.4 mg/ml Papain (Worthington), 1 mg/ml BSA (Sigma) and 1 mg/ml DTT (Sigma) and incubated at 37 °C for 20 min in a shaking water bath. After two washings in SMDS 10µM Ca<sup>2+</sup> a second 25 min incubation was performed with SMDS 10µM Ca<sup>2+</sup> in a 0.28 mg/ml collagenase F, 0.12 mg/ml collagenase H (Sigma) and 1 mg/ml BSA solution. Single cells were obtained by gentle trituration with a wide-bore glass pipette, stored at 4 °C and used within the same day. Ionic composition of SMDS was (in mM): NaCl 145; KCl 4.2; KH<sub>2</sub>PO<sub>4</sub> 0.6; MgCl<sub>2</sub> 1.2; Hepes 10; Glucose 11. pH was adjusted to 7.4 with NaOH.

For the isolation of VSMCs from injured arteries, a different dissociation protocol was employed, based on a previously described method<sup>2</sup>. Briefly, after careful dissection of connective tissue, small pieces of artery were placed in 200 µL of culture media (D-MEM medium supplemented with 10% FBS, penicillin-streptomycin (100 U/ml each), 5 µg/ml fungizone and 2 mM L-glutamine) containing 1.36 mg/ml collagenase type I (Worthington), and left in the incubator (at 37 °C in a 5% CO<sub>2</sub> humidified atmosphere) for four to six hours. After that, 3 ml of culture media were added and cells were transfer to a conical tube and centrifuged for 5 min at 300xg. The pellet was resuspended in a small volume of culture medium and dispersed cells were plated onto poly-L-lysine coated coverslips with 2ml of culture medium supplemented with 1% FBS and maintained in the incubator.

Electrophysiological experiments were performed within 4-24h after isolation. Parallel studies were performed with VSMCs isolated from contralateral control arteries to confirm that the isolation and culture conditions did not modify the expression pattern of ion channels observed in acutely dispersed VSMCs.

### ***VSMCs culture***

After carefully dissection and cleaning of connective and endothelial tissues, small pieces of femoral, mesenteric or uterine arteries were placed in a 35 mm culture dish covered with 2 % gelatin (Type B from bovine skin, Sigma) in DMEM supplemented with 20 % SFB, penicillin-streptomycin (100 U/ml each), 5 µg/ml fungizone, and 2 mM L-glutamin (Lonza) at 37 °C in a 5% CO<sub>2</sub> humidified atmosphere. Migration and proliferation of VSMCs from the explants was evident within 6-10 days. When cells reached confluence, they were detached by exposure to trypsin-EDTA (Lonza) during 3-7 minutes followed by mechanical scraping with a rubber spatula. They were then seeded in a new culture plate at a 1/3 density in SMC-P-STIM medium: D-MEM medium supplemented with 5% FBS, penicillin-streptomycin (100 U/ml each), 5 µg/ml fungizone, L-glutamine (2 mM), Insulin (5 µg/ml), bFGF (2

ng/ml) and EGF (0.5 ng/ml). VSMCs were subjected to several (3-4) passages without showing morphological changes.

To determine the effect of membrane depolarization on femoral VSMCs proliferation rate, cells were placed in culture media with increased K<sup>+</sup> concentrations (5, 10 and 20 mmol/L). These media were reconstituted with MEM amino acids solution (M5550, Sigma), MEM non-essential amino acid solution (M7145, Sigma), MEM Eagle vitamin mix (13-607C, [BioWhittaker®](#)) and a buffer composition identical to DMEM, except that Na<sup>+</sup> and K<sup>+</sup> concentrations were varied to maintain osmolarity. In all cases, parallel experiments were carried out using the control medium (SMC-P-STIM) as a control of the 5 mM K<sup>+</sup>-reconstituted medium.

### **RNA Isolation, RT and real time PCR**

Total RNA from arteries was isolated with MELT™ Total RNA Isolation System Kit (Ambion) as previously described<sup>3</sup>. 6-10 femoral arteries (or 20-30 mesenteric arteries or 5-6 aorta arteries) were employed for each determination. Total RNA from cultured VSMCs and HEK293 cells were isolated with Trizol Reagent (Invitrogen) using 3-5 35 mm culture dishes with cells closed to confluency. In the case of cultured VSMCs, we used cells proceeding from several arteries from different animals for each experiment. The quality of the RNA was assayed by OD measurement at 260 and 280 nm and by electrophoresis on agarose gels. After DNase I (Ambion) treatment, 500-750 ng of RNA were reverse transcribed with 5000 u/ml of MuLVRT in the presence of 20 u/μl of RNase inhibitor, 50 μM Random Hexamers, 10X PCR buffer, 25 mM MgCl<sub>2</sub> and 10 mM mixed dNTPs at 42 °C for 60 min, to get cDNA (RT+). All reagents were from Applied Biosystems. From the same samples, 200-350 ng of total RNA were used as genomic control in reverse transcriptase reaction in the absence of MuLVRT and RNase Inhibitor at 42 °C for 60 min (RT-). A small fraction of these cDNAs was used for real-time amplifications of selected control genes (Gapdh and Gusb) to compare the different samples, and also, given the intronless nature of the mGapdh gene, to check the efficiency of the DNase treatment by comparing expression levels of the gene between RT+ and RT- samples.

The mRNA expression levels were determined by real-time PCR in a Rotor-Gene 3000 (Corbett Research) thermocycler using TaqMan® Gene Expression Assays or SYBR Green I with PCR primer sets designed with the Primer 3 website ([http://frodo.wi.mit.edu/cgi-bin/primer3/primer3\\_www.cgi](http://frodo.wi.mit.edu/cgi-bin/primer3/primer3_www.cgi)).

Real-time PCR with TaqMan Low Density Arrays (Applied Biosystems) was carried out by the Genomic Service of the CNIC (Madrid, Spain), with the ABI Prism 7900HT Sequence detection system (Applied Biosystems) and data were acquired with SDS 2.1 software. mRNA expression levels were determined using the threshold cycle (Ct) relative quantification method ( $\Delta\Delta Ct$ )<sup>4</sup>.

Expression data of genes were normalized by an internal control, ribosomal (RNA 18s, Gapdh or Gusb). The relative abundance of the genes was calculated from  $2^{(-\Delta Ct)}$ , where

$$\Delta Ct = Ct_{gen} - Ct_{internal\ control}$$

Changes in the expression between control (calibrator) and the different experimental conditions were calculate from  $2^{(-\Delta\Delta Ct)}$ , where

$$\Delta\Delta Ct = \Delta Ct_{experimental} - \Delta Ct_{calibrator}$$

In order to do statistical comparisons,  $\Delta Ct$  values obtained in each sample, ( $Ct_{gen} - Ct_{internal\ control}$ ), were subtracted from the mean  $\Delta Ct$  of the calibrator to provide the SE. In the cases in which expression of a gene was not detected in one of the conditions, a Ct value of 40 was assigned in order to do the comparisons.

Primers, TaqMan probes and TaqMan® Gene Expression Assays (Applied Biosystems) used (the list of genes studied with the Taqman® Low Density Arrays is provided in Table I):

*mGapdh*: 5'-TGTGTCCGTCGTGGATCTG-3', 5'- GATGCCTGCTTCACCACTT-3' and 5'-FAM-TGGAGAAACCTGCCAAGTATGATGACATCA-BHQ2-3';

*mGusb*: 5'-CAATGGTACCGGCAGCC-3', 5'-AAGCTAGAAGGGACAGGCATGT-3' and 5'-FAM-TACGGGAGTCGGGCCAGTCTTG-BHQ2-3'.

*mCnn1*: 5'-ACAAGAGCGGAGATTTGAGC-3' and 5'-TGAGTGTGTGCGAGTGTTC-3'

*meNos*: 5'-GCATCACCAGGAAGAAGACC-3' and 5'-GGGACACCACATCATACTCATC-3'

*hGUSB*: 5'-ACCAGGGACCATCCAATACC-3' and 5'-CATCCAAAAGACGCACTTCC-3'

*mKcna3*: Mm00434599\_s1

*hCNN1*: Hs00154543\_m1

## Data analysis

Data from the TaqMan® Low Density Arrays were analyzed with several independent methods. A two-way hierarchical clustering was applied to the gene-expression matrix consisting on the cards of the different conditions explored and the genes with significant expression in at least one of the experimental conditions. The values introduced for each gene were the  $\Delta Ct$  of each experiment (the mean  $\Delta Ct$  of the duplicates). We used the Cluster software<sup>5</sup> and applied average linkage clustering with uncentered correlation after array normalization. Clusters were visualized using the Treeview software. Relationships among genes are represented by a tree whose branch lengths reflect their degree of similarity assessed by a pairwise similarity function. The computer trees are used to order the genes in the original data table, so that groups of genes with similar expression pattern are adjacent. When this ordered table is displayed graphically, the presence of contiguous patches of colour can be readily identified. A second method of analysis was the determination in each experimental conditions of the relative expression of each gene to obtain its  $2^{(-\Delta Ct)}$  value. The averaged (mean  $\pm$  SEM)  $\Delta Ct$  values for each gene in control versus proliferative conditions were used to obtain the differences in expression ( $2^{(-\Delta \Delta Ct)}$ ) between both conditions as indicated above, and statistical differences were determined with a student t-test. Finally, the  $\Delta Ct$  values of all the genes from each array were compared in the different situations with an analysis of variance (in the case of endoluminal lesion) or a t-test (in the case of cultured femoral VSMCs) to test for mean differences between the groups. The obtained p-values were adjusted for multiple testing with the false discovery rate (FDR) control<sup>6</sup> using the tools for differential gene expression of the suite of programs GEPAS (<http://gepas.bioinfo.cipf.es/>). The choice of a high enough posterior probability of differential expression is considered to control for the multiplicity of tests performed.

## ***Histology and immunohistochemistry***

For the morphometric and immunohistochemical analysis, animals were euthanized 48 hours, 1 and 4 weeks after arterial injury and perfusion-fixed with 4% paraformaldehyde in PBS for 5 min at 100 mmHg to obtain paraffin sections from femoral arteries as described in previous studies<sup>1</sup>. Three 5- $\mu$ m-thick paraffin sections from each arterial segment were stained with combined Masson's trichrome elastic and analyzed by using computerized morphometry (NIH Image) and the average values were calculated. Measurements included luminal area, medial area, intimal area, vessel area, and the lengths of the internal elastic lamina and external elastic lamina. From these data, the intima-to-media (I/M) ratio (IA/MA), and the percentage of luminal stenosis ( $100 \cdot IA / (LA + IA)$ ) was calculated as previously described<sup>1</sup>. The percentage of stenosis obtained were  $35 \pm 7.24\%$  for 1 week after lesion and  $75.64 \pm 4.82$  for 4 weeks after lesion.

For immunohistochemical analysis, paraffin sections were deparaffined, rehydrated, treated with 1% citric acid for antigen retrieval and blocked with 3% hydrogen peroxide (DakoCytomatation) before the incubation with primary antibodies at 4°C ON. Sections were washed in PBS, incubated with a horseradish peroxidase conjugated anti-mouse IgG (DakoCytomatation) for 30 minutes at room temperature (RT). Signal was detected using 3,3-diaminobenzidine (DAB, DakoCytomatation). After being washed in distilled water, all sections were counterstained with hematoxylin. Negative controls were prepared by substitution of the primary antibody with an irrelevant antibody. Primary antibodies used were: mouse anti-Kv1.3 (clone L23/27) and mouse anti-Kv1.5 (clone K7/45) both from Neuromab (UC Davis NIH and Antibodies Inc.). Immunohistochemical measurements were performed as follows: four magnified (x 20) areas of the vessel wall, acquired from each of the four quadrants of the arterial circumference, were blindly analyzed (Image AnalySIS 2.3). The percentage of labelled area over the total vessel area was calculated for all arteries.

## ***Immunocytochemistry***

Freshly isolated VSMCs plated onto glass coverslips were allowed to set for 30 min at RT, and cultured VSMCs were directly seed in coverslips placed in the bottom of petri dishes 2-3 days before the immunofluorescence assay. Cells were fixed with 4% paraformaldehyde (PF) in phosphate buffer, pH 7.5, for 15 min at 20 °C, washed in PBTx (PBS, 0.1% Triton X-100), and blocked with PBTx with 2% of normal goat serum for 10 min. Primary antibodies were diluted in blocking solution and incubated with the cells for 60 min at RT at final dilutions indicated below. After washes in PBTx, cells were incubated with secondary antibodies for 30 min. The fluorescently labelled secondary antibodies (Alexa 488 goat anti-mouse/rabbit secondary antibodies -Molecular Probes-) were used at a final dilution of 1:1000. After washes in PBS, the coverslips were mounted with Vectashield H-1000 (Vector Labs) with DAPI, and photomicrographs were acquired with Nis-element software (Nikon).

The primary antibodies used and their final dilution were: mouse anti-Kv1.3 (1:33, NeuroMab, Antibodies Inc.), rabbit anti-Kv1.5 (1:50, Sigma), mouse anti-SM $\alpha$ A (1:100), rabbit anti-Calponin (1:50) and anti-SM22 (1:50) (abcam, ab7817, ab46794 and ab14106 respectively).

## ***Electrophysiological methods***

Ionic currents were recorded at RT (20-25 °C) using the whole-cell configuration of the patch-clamp technique as previously described<sup>3,7</sup>. The coverslips with the attached cultured VSMCs were placed at the bottom of a small recording chamber (0.2 ml) on the stage of an inverted microscope and perfused by gravity with the bath solution, while freshly isolated VSMCs were placed directly on the recording chamber and let to sit for a few minutes before starting superfusion with the external solution. Patch pipettes were made from borosilicate glass (2.0 mm O.D., WPI) and double pulled (Narishige PP-83) to resistances ranging from 7 to 10 MΩ for VSMCs when filled with an internal solution, containing (mM): 125 KCl, 4 MgCl<sub>2</sub>, 10 HEPES, 10 EGTA, 5 MgATP; (pH 7.2 with KOH). The composition of the bath solution was (mM): 141 NaCl, 4.7 KCl, 1.2 MgCl<sub>2</sub>, 1.8 CaCl<sub>2</sub>, 10 glucose, 10 HEPES, (pH 7.4 with NaOH). Whole-cell currents were recorded using an Axopatch 200 patch-clamp amplifier, filtered at 2 kHz (-3 dB, 4-pole Bessel filter), and sampled at 10 kHz. When leak-subtraction was performed, an online P/4 protocol was used. Recordings were digitized with a Digidata 1200 A/D interface, driven by CLAMPEX 8 software (Axon Instruments) in a Pentium clone computer.

Current-voltage relationships were obtained from a holding potential of -80 mV in 10 mV depolarizing steps from -60 to +80 mV during 200 ms. Paxilline, tetraethylammonium chloride (TEA) and PAP-1 were obtained from Sigma, Margatoxin and Stromatoxin were from Alomone Labs, and correolide was a gift from Dr. María García (Merck).

Electrophysiological data analyses were performed with the CLAMPFIT subroutine of the PCLAMP software (Axon) and with ORIGIN 7.5 software (Microcal Inc.). Pooled data are expressed as mean ± standard error of the mean (SEM). Statistical comparisons between groups of data were carried out with the two-tailed Student t test for paired or unpaired data, and values of p < 0.05 were considered statistically different.

Membrane potential ( $V_M$ ) measurements were performed at RT using the perforated-patch technique to avoid dialysis of intracellular medium. For these experiments, recordings were obtained with an Axopatch 4A patch-clamp amplifier. Pipette tips were briefly dipped into a solution containing (in mM): 40 KCl, 95 KGlutamate, 8 CaCl<sub>2</sub>, 10 HEPES, pH 7.2 with KOH, and backfilled with the same solution containing amphotericin B (480 µg/ml). After obtaining a high-resistance seal, electrical access to cell cytoplasm was assessed by monitoring the increase in cell capacitance. At this point, the amplifier was switched to current-clamp mode and membrane potential was continuously recorded. The high Ca<sup>2+</sup> content of the pipette solution ensures the correct performance of the perforate-patch technique, as accidental rupture of the patch (changing to whole-cell configuration) would lead to a sudden Ca<sup>2+</sup> load and cell death. The composition of the bath solution was the same that the indicated for the voltage-clamp experiments, except for the experiments exploring the effect of high extracellular K<sup>+</sup>, in which Na<sup>+</sup> concentration in the external solution was reduced equimolarly.

## ***Cell Migration assay***

To evaluate migration we used a wound healing or scratch assay<sup>8</sup>, in cultured VSMCs from mouse femoral arteries. Cells were seeded in 4-well plates (1.8 cm<sup>2</sup>/well) and grown in SMC-P-STIM medium until confluence. Monolayers were manually scraped with a 200 µl pipette tip, gently washed three

times with PBS to remove non-adherent cells, and incubated in a serum free medium (SF medium) to block proliferation. The SF medium is a DMEM supplemented with 500 nM insulin, 5 µg/ml transferrin 100 U/ml each penicillin and streptomycin, 5 µg/ml fungizone, and 2 mM L-glutamine. Images of the scratched area were taken immediately (time 0) and 24 hours after injury. The scratched area was measured using Image J software. Percentage of invaded area was determined as

$$\% \text{ Reinvansion} = 100 \cdot (\text{Area}_0 - \text{Area}_{24}) / \text{Area}_0$$

where  $\text{Area}_0$  = initial area (t=0) and  $\text{Area}_{24}$  = area at time 24 h after injury.

Migration assays were performed in the absence (control) or presence of 10 nM PAP-1 or margatoxin.

### **Proliferation assays**

Femoral, mesenteric or uterine cultured VSMCs were plated in poli-L-lysine coated coverslips and grown to approximately 65-80 % confluence. At this point, cells were synchronized by incubation during 48-72 h in SF medium at 37 °C in a 5% CO<sub>2</sub> humidified atmosphere. After this, cells were either maintained in SF medium (negative control), placed in SMC-P-STIM medium alone (control) or SMC-P-STIM medium with 10 nM Margatoxin, 10 nM PAP-1, 50 nM Stromatoxin, 500 nM Paxilline or culture media with high (10 or 20 mM) K<sup>+</sup> concentrations (experimental conditions) during 24h. At the end of this period, BrdU incorporation assay were performed by incubation with the BrdU labeling medium for 60 min at 37 °C in a 5% CO<sub>2</sub> humidified atmosphere and then fixed with 50 mM glycine solution in 70% ethanol for 20 min at -20 °C. Incorporated BrdU was detected by 30 min incubation at 37°C with anti-BrdU, followed by 30 min incubation at 37°C with anti-mouse-Ig-fluorescein, according to manufacturer's instructions (Roche Applied Science, Germany). Coverslips were mounted in Vectashield with DAPI (Vector Laboratories, INC., Burlingame, CA), and BrdU incorporation was measured and represented as the percentage of BrdU positive cells (BrdU<sup>+</sup>) from the total cell number stained with DAPI. In each experiment, BrdU incorporation was obtained from the average of at least 10 different fields for each condition.

### **siRNA transfections**

Femoral cultured VSMCs were plated in poli-L-lysine coated coverslips in 4-well plates (1.8 cm<sup>2</sup>/well, Nunc™) at 60%–70% confluence. Cells were incubated in SF medium 24 h prior to transfection. Transfections were performed using 35 nM of siRNA (Applied Biosystems) and 1.2 µl of Lipofectamine™ 2000 (Invitrogen) following manufacturer instructions, 24h after transfection cells were placed in SMC-P-STIM medium at 37 °C in a 5% CO<sub>2</sub> humidified atmosphere. A high transfection efficiency (>80%) was determined by transfection with BLOCK-iT™ Fluorescent oligo (Invitrogen), and detection of the fluorescence signal at 24 h post-transfection using fluorescence microscopy. siRNA validations were performed in culture femoral cells that were either mock-transfected (control), transfected with negative control siRNA or with siRNA against Kv1.3. The reduction in the expression of Kv1.3 upon siRNA transfection was evaluated at 48h post-transfection at the mRNA level by quantitative PCR, using Gapdh as housekeeping and mock-transfected cells as calibrator. The Kv1.3 siRNA tested were: s68583 (siRNA1), s68585 (siRNA2) and the siRNA negative control 4390843 (Applied Biosystems). BrdU incorporation was determined 48 h post- transfection.

## ADDITIONAL FIGURES AND SUPPORTING INFORMATION

### *List of genes studied with the Taqman® low-density array*

The list of the genes whose expression was explored in this study is provided in Table I. The information provided includes the gene name (the nomenclature used through the paper), the gene symbol, the Applied Biosystem ID of the Taqman® assay and the Genbank accession number of the nucleotide sequence. The array lacks some  $\alpha$  and  $\beta$  subunits of the  $K^+$  channel family, as well as some  $\alpha$  subunits of other channel families studied (i.e. Trp channels or  $Cl^-$  channels) due to the fact that they were not available as inventoried Taqman® assays at the moment this study started.

**Table I. Genes explored in the study**

Gene Name	Gene Symbol	Assay ID	NCBI Gene Ref	Category
18S RNA	18SRNA	Hs99999901_s1	X03205.1	endogenous control
SUR2	Abcc9	Mm00441638_m1	NM_011511.1,NM_021041.1,	$K^+$ channel
B2m	B2m	Mm00437762_m1	NM_009735.2	endogenous control
Cav1.2	Cacna1c	Mm00437917_m1	NM_009781.1	$Ca^{2+}$ channel
Cav1.3	Cacna1d	Mm00551384_m1	NM_028981.1	$Ca^{2+}$ channel
Cav3.1	Cacna1g	Mm00486549_m1	NM_009783.1	$Ca^{2+}$ channel
Cav3.2	Cacna1h	Mm00445369_m1	NM_021415.3	$Ca^{2+}$ channel
Cav1.1	Cacna1s	Mm00489257_m1	AW493108	$Ca^{2+}$ channel
Clca1	Clca1	Mm00777368_m1	NM_009899.2	$Cl^-$ channel
Clca2	Clca2	Mm00661630_m1	NM_030601.2	$Cl^-$ channel
Clca3	Clca3	Mm00489959_m1	NM_017474.1	$Cl^-$ channel
Clca4	Clca4	Mm00519742_m1	NM_139148.1	$Cl^-$ channel
Clca5	Clca5	Mm00724513_m1	NM_178697.3	$Cl^-$ channel
Clcn3	Clcn3	Mm00432566_m1	NM_173876.2,NM_007711.2	$Cl^-$ channel
Cnn1	Cnn1	Mm00487032_m1	NM_009922.2	cytoskeletal protein
Gapdh	Gapdh	Mm99999915_g1	NM_001001303.1	endogenous control
Hprt1	Hprt1	Mm00446968_m1	NM_013556.2	endogenous control
Kv1.1	Kcna1	Mm00439977_s1	NM_010595.2	$K^+$ channel
Kv1.2	Kcna2	Mm01546131_g1	NM_008417.2	$K^+$ channel
Kv1.3	Kcna3	Mm00434599_s1	NM_008418.1	$K^+$ channel
Kv1.4	Kcna4	Mm01336166_m1	NM_021275.2	$K^+$ channel
Kv1.5	Kcna5	Mm00524346_s1	NM_145983.1	$K^+$ channel
Kv1.6	Kcna6	Mm00496625_s1	NM_013568.4	$K^+$ channel
Kvbeta1	Kcnab1	Mm00440018_m1	NM_010597.2	$K^+$ channel
Kvbeta2	Kcnab2	Mm00440022_m1	NM_010598.2	$K^+$ channel
Kvbeta3	Kcnab3	Mm00440034_g1	NM_010599.2	$K^+$ channel
Kv2.1	Kcnb1	Mm00492791_m1	NM_008420.3	$K^+$ channel
Kv3.1	Kcnc1	Mm00657708_m1	NM_008421.2	$K^+$ channel
Kv3.3	Kcnc3	Mm00434614_m1	NM_008422.1	$K^+$ channel
Kv3.4	Kcnc4	Mm00521443_m1	NM_145922.1	$K^+$ channel
Kv4.1	Kcnd1	Mm00492796_m1	NM_008423.1	$K^+$ channel
Kv4.2	Kcnd2	Mm00498065_m1	NM_019697.3	$K^+$ channel
Kv4.3	Kcnd3	Mm00498260_m1	NM_019931.1	$K^+$ channel
Mink	Kcne1	Mm00434615_m1	NM_008424.3, X60457.1	$K^+$ channel
MiRP1	Kcne2	Mm00506492_m1	NM_134110.1	$K^+$ channel
MiRP2	Kcne3	Mm00445119_m1	NM_020574.3	$K^+$ channel
Kv6.3	Kcng3	Mm00463328_m1	NM_153512.1	$K^+$ channel
Kv10.1	Kcnh1	Mm00495110_m1	NM_010600.2	$K^+$ channel
Kv11.1(erg-1)	Kcnh2	Mm00465370_m1	NM_013569.1	$K^+$ channel
Kv11.3(erg-3)	Kcnh7	Mm00713030_m1	NM_133207.1	$K^+$ channel
KChIP1	Kcnip1	Mm00471928_m1	NM_027398.2	$K^+$ channel

KChIP2	Kcnip2	Mm00518914_m1	NM_030716.2,NM_145703.1	K <sup>+</sup> channel
KChIP3	Kcnip3	Mm00490739_m1	NM_019789.2	K <sup>+</sup> channel
KChIP4	Kcnip4	Mm00518835_m1	NM_030265.2	K <sup>+</sup> channel
Kir4.1	Kcnj10	Mm00444727_s1	NM_019659.2	K <sup>+</sup> channel
Kir6.2	Kcnj11	Mm00445028_m1	NM_001039484.1	K <sup>+</sup> channel
Kir2.2	Kcnj12	Mm00440050_s1	NM_010602.2	K <sup>+</sup> channel
Kir1.1	Kcnj1	Mm01237201_m1	NM_010603.3	K <sup>+</sup> channel
Kir2.1	Kcnj2	Mm00434616_m1	NM_008425.2	K <sup>+</sup> channel
Kir3.1	Kcnj3	Mm00434618_m1	NM_008426.1	K <sup>+</sup> channel
Kir3.2	Kcnj6	Mm00440070_m1	NM_001025584.2, NM_010606.2	K <sup>+</sup> channel
Kir6.1	Kcnj8	Mm00434620_m1	NM_008428.2	K <sup>+</sup> channel
Kir3.3	Kcnj9	Mm00434622_m1	NM_008429.2	K <sup>+</sup> channel
TWIK1	Kcnk1	Mm00434624_m1	NM_008430.1	K <sup>+</sup> channel
TREK1	Kcnk2	Mm00440072_m1	NM_010607.1	K <sup>+</sup> channel
TASK1	Kcnk3	Mm00807036_m1	NM_010608.2	K <sup>+</sup> channel
TRAAK	Kcnk4	Mm00434626_m1	NM_008431.1	K <sup>+</sup> channel
TASK2	Kcnk5	Mm00498900_m1	NM_021542.2	K <sup>+</sup> channel
BK	Kcnma1	Mm00516078_m1	NM_010610.2	K <sup>+</sup> channel
BKbeta1	Kcnmb1	Mm00466621_m1	NM_031169.2	K <sup>+</sup> channel
BKbeta2	Kcnmb2	Mm00511481_m1	NM_028231.2	K <sup>+</sup> channel
BKbeta4	Kcnmb4	Mm00465684_m1	NM_021452.1	K <sup>+</sup> channel
SK1	Kcnn1	Mm00446259_m1	NM_032397.1	K <sup>+</sup> channel
SK2	Kcnn2	Mm00446514_m1	NM_080465.1	K <sup>+</sup> channel
SK3	Kcnn3	Mm00446516_m1	NM_080466.1	K <sup>+</sup> channel
SK4(IK1)	Kcnn4	Mm00464586_m1	NM_008433.2	K <sup>+</sup> channel
Kv9.1	Kcns1	Mm00492824_m1	NM_008435.2	K <sup>+</sup> channel
Kv9.2	Kcns2	Mm00492825_g1	NM_181317.3	K <sup>+</sup> channel
Kv9.3	Kcns3	Mm00557826_m1	NM_173417.1	K <sup>+</sup> channel
Klf5	Klf5	Mm00456521_m1	NM_009769.2	proliferation marker
Nos3	Nos3	Mm00435204_m1	NM_008713.2	endotelial cell marker
KChAP	Pias3	Mm00450739_m1	NM_146135.1,NM_018812.1	K <sup>+</sup> channel
Trpp1	Pkd1	Mm00465434_m1	NM_013630.1	TRP channel
Trpp2	Pkd2	Mm00435829_m1	NM_008861.2	TRP channel
Trpp5	Pkd2l2	Mm00450423_m1	NM_016927.1	TRP channel
Trpc1	Trpc1	Mm00441975_m1	NM_011643.1	TRP channel
Trpc2	Trpc2	Mm00441984_m1	NM_011644.1	TRP channel
Trpc3	Trpc3	Mm00444690_m1	NM_019510.1	TRP channel
Trpc4	Trpc4	Mm00444284_m1	NM_016984.1	TRP channel
Trpc5	Trpc5	Mm00437183_m1	NM_009428.1	TRP channel
Trpc6	Trpc6	Mm00443441_m1	NM_013838.1	TRP channel
Trpc7	Trpc7	Mm00442606_m1	NM_012035.1	TRP channel
Trpm1	Trpm1	Mm00450619_m1	NM_018752.2	TRP channel
Trpm2	Trpm2	Mm00663098_m1	NM_138301.1	TRP channel
Trpm3	Trpm3	Mm00616485_m1	NM_177341.3	TRP channel
Trpm4	Trpm4	Mm00613173_m1	NM_175130.2	TRP channel
Trpm5	Trpm5	Mm00498453_m1	NM_020277.1	TRP channel
Trpm6	Trpm6	Mm00463112_m1	NM_153417.1	TRP channel
Trpm7	Trpm7	Mm00457998_m1	NM_021450.1	TRP channel
Trpm8	Trpm8	Mm00454566_m1	NM_134252.2	TRP channel
Trpv2	Trpv2	Mm00449223_m1	NM_011706.1	TRP channel
Trpv3	Trpv3	Mm00454996_m1	NM_145099.1	TRP channel
Trpv4	Trpv4	Mm00499025_m1	NM_022017.1	TRP channel
Trpv6	Trpv6	Mm00499069_m1	NM_022413.2	TRP channel
Vwf	Vwf	Mm00550376_m1	NM_011708.2	endotelial cell marker

## ***Statistical analysis of the differential gene expression in the two proliferation models***

As mentioned above, several independent methods have been used to analyze the data obtained in the low density Taqman<sup>®</sup> arrays. First we analyzed the differences in expression for each individual gene. In this case,  $\Delta\text{Ct}$  values for each gene in control (contractile) conditions were used as calibrator, and the fold-change upon proliferation was calculated using the  $2^{(-\Delta\Delta\text{Ct})}$  relative quantification method<sup>4</sup>. Significant changes in expression were determined with a student t-test (in the case of in vitro proliferation) or with an Anova test (for the in vivo lesions at different time points). Genes showing statistically significant changes in their expression are shown in Figure III in which the log of  $2^{(-\Delta\Delta\text{Ct})}$  was used for representing the data, so that a value of 0 means no change, positive values represent increased expression and negative values decreased expression.

A different analysis method was used for the diagram shown in figure 2C, that has been constructed from the output of the statistical analysis of the data in GEPAS suite. The T-Rex set of programs (used for analyzing differential gene expression) provides estimates for statistics, p-values and posterior probabilities that are used to order genes in terms of their pattern of differential expression. When appropriate, p-values adjusted for multiple testing are provided, and in this case, three methodologies are implemented. One of them, the method proposed by Holm (fwer.holm) controls the FWER (family-wise error rate). The other two methods control the FDR (false discovery rate), one using the algorithm proposed by Benjamini & Hochberg<sup>9</sup> (fdrBH) and the other one implementing the q values method proposed by Storey<sup>10</sup>.

The following tables show all the data provided by this analysis in the two conditions explored: Differential gene expression when comparing tissue versus cultured VSMCs (Table II) and differential gene expression in the endoluminal lesion at different times, by using multi-class option in T-Rex (Table III). The first analysis uses an statistical method based on t-test, where increased and decrease expression are indicated with positive and negative values on the column labelled as "statistic", while in the second approach the differential gene expression was evaluated by an Anova test and all the statistic values are positive regardless of whether they reflect increased or decreased expression referred to the control data. In both analysis, we selected genes (shown in bold) showing a fdrBH correction of the p-value below 0.05.

**Table II- Statistics of the differential gene expression in the cultured VSMCs**

genename	Statistic	pvalue	fwer.holm	fdrBH	Q value
<b>Kvbeta2</b>	<b>8.17370701</b>	<b>0.00121993</b>	0.0646563	<b>0.00780945</b>	6.57E-05
<b>Kv3.3</b>	<b>7.8563261</b>	<b>0.00141828</b>	0.07233232	<b>0.00780945</b>	6.57E-05
<b>Kv1.4</b>	<b>5.95294952</b>	<b>0.00399612</b>	0.17982556	<b>0.01445634</b>	0.00012155
<b>TREK1</b>	<b>5.57012415</b>	<b>0.00508973</b>	0.21885853	<b>0.01628148</b>	0.0001369
<b>Kv10.1</b>	<b>5.25077105</b>	<b>0.0062939</b>	0.24546191	<b>0.01716517</b>	0.00014433
<b>Kir2.1</b>	<b>3.83103347</b>	<b>0.01860164</b>	0.61385403	<b>0.03986065</b>	0.00033515
<b>Kv1.3</b>	<b>3.64932156</b>	<b>0.02178451</b>	0.69710434	<b>0.0448444</b>	0.00037706
Kv4.1	3.29808426	0.02998722	0.86962937	0.05622604	0.00047276
Trpp2	2.58948827	0.06071666	1	0.10851494	0.00091241
Kv11.1(erg-1)	2.57746506	0.0614918	1	0.10851494	0.00091241
Cav1.3	1.95279861	0.1225629	1	0.18855831	0.00158543
Trpm7	1.79068255	0.14783308	1	0.22174962	0.0018645
Trpc4	1.69386196	0.16554163	1	0.24225605	0.00203692
SK3	1.61822724	0.18092404	1	0.25245215	0.00212265
SK4(IK1)	1.53536665	0.19949053	1	0.27203254	0.00228729
KChIP4	1.3463968	0.24941032	1	0.31839615	0.00267712
Clca1	1.23468828	0.28451884	1	0.34839041	0.00292932
Kvbeta3	1.14244211	0.31700847	1	0.38041016	0.00319854
BKbeta2	0.99427581	0.37636554	1	0.44278299	0.00372298
Kv4.2	0.90677834	0.41580963	1	0.47978034	0.00403406
Kv11.3(erg-3)	0.67404014	0.53723198	1	0.59692442	0.00501903
BKbeta4	0.59900737	0.58144152	1	0.63429984	0.00533328
Clcn3	0.42667291	0.6915791	1	0.71593862	0.00601971
Trpm4	0.42593554	0.692074	1	0.71593862	0.00601971
Trpc6	0.37996328	0.72328609	1	0.73554518	0.00618457
Trpc3	-0.21835274	0.83784199	1	0.83784199	0.00704469
TASK2	-0.45515728	0.67260641	1	0.71593862	0.00601971
Cav3.1	-0.82275116	0.45686874	1	0.51720989	0.00434877
Kir2.2	-1.29922712	0.26369187	1	0.32961484	0.00277145
Trpm3	-1.39990246	0.23412763	1	0.30538386	0.00256771
Trpp1	-1.51286447	0.20486273	1	0.2731503	0.00229669
Trpv4	-1.66192031	0.17186399	1	0.24551998	0.00206437
Trpc1	-2.20678592	0.09195467	1	0.14519159	0.00122079
SK1	-2.2110281	0.0915213	1	0.14519159	0.00122079
Kvbeta1	-2.23344564	0.08926876	1	0.14519159	0.00122079
Kv1.6	-2.27333283	0.0854127	1	0.14519159	0.00122079
KChAP	-3.33552337	0.02895622	0.86868664	0.0560443	0.00047123
<b>Cav3.2</b>	<b>-3.61672854</b>	<b>0.0224222</b>	0.69710434	<b>0.0448444</b>	0.00037706
<b>Kir6.2</b>	<b>-3.90818429</b>	<b>0.01742053</b>	0.59229797	<b>0.03871229</b>	0.0003255
<b>SK2</b>	<b>-4.00756454</b>	<b>0.01602898</b>	0.56101442	<b>0.03698996</b>	0.00031102
<b>BK</b>	<b>-4.42333794</b>	<b>0.01148113</b>	0.41332077	<b>0.02755472</b>	0.00023168
<b>SUR2</b>	<b>-4.56965876</b>	<b>0.01026344</b>	0.37974736	<b>0.02565861</b>	0.00021574
<b>Trpv2</b>	<b>-4.8159337</b>	<b>0.00854828</b>	0.32483479	<b>0.02229987</b>	0.0001875
<b>Kv9.3</b>	<b>-5.31708384</b>	<b>0.00601738</b>	0.2406952	<b>0.01716517</b>	0.00014433
<b>Kv2.1</b>	<b>-5.47198963</b>	<b>0.00542716</b>	0.22251359	<b>0.01628148</b>	0.0001369
<b>TASK1</b>	<b>-5.52488279</b>	<b>0.005242</b>	0.22016411	<b>0.01628148</b>	0.0001369
<b>Trpc2</b>	<b>-5.91292953</b>	<b>0.00409596</b>	0.18022234	<b>0.01445634</b>	0.00012155
<b>Kv1.5</b>	<b>-6.12597418</b>	<b>0.00359737</b>	0.16547902	<b>0.01438948</b>	0.00012099
<b>Cnn1</b>	<b>-6.4240303</b>	<b>0.00301876</b>	0.14271396	<b>0.01293754</b>	0.00010878
<b>Kv1.1</b>	<b>-6.45044422</b>	<b>0.00297321</b>	0.14271396	<b>0.01293754</b>	0.00010878
<b>Nos3</b>	<b>-7.83681488</b>	<b>0.00143173</b>	0.07233232	<b>0.00780945</b>	6.57E-05
<b>Cav1.2</b>	<b>-8.04425144</b>	<b>0.0012964</b>	0.06741296	<b>0.00780945</b>	6.57E-05
<b>Kir6.1</b>	<b>-8.41477966</b>	<b>0.00109184</b>	0.05895932	<b>0.00780945</b>	6.57E-05
<b>TWIK1</b>	<b>-8.71250629</b>	<b>0.0009558</b>	0.05256908	<b>0.00780945</b>	6.57E-05
<b>Kir4.1</b>	<b>-9.92673874</b>	<b>0.00057823</b>	0.03238081	<b>0.00693875</b>	5.83E-05
<b>Kv4.3</b>	<b>-10.3333073</b>	<b>0.00049494</b>	0.02821165	<b>0.00693875</b>	5.83E-05
<b>Kv3.4</b>	<b>-11.7948427</b>	<b>0.0002957</b>	0.01715064	<b>0.00591401</b>	4.97E-05
<b>Kv1.2</b>	<b>-14.4185619</b>	<b>0.00013448</b>	0.00793443	<b>0.00403445</b>	3.39E-05
<b>BKbeta1</b>	<b>-16.6256809</b>	<b>7.67E-05</b>	0.00460026	<b>0.00403445</b>	3.39E-05

**Table III- Statistics of the differential gene expression in the endoluminal lesion**

genename	Statistic	pvalue	fwer.holm	fdrBH	Q value
Clca1	68.422699	4.80E-06	0.00028793	0.00028793	7.85E-05
Kv1.5	37.1956978	4.79E-05	0.00282894	0.00143845	0.00039215
Kv2.1	30.5888004	9.84E-05	0.00570879	0.00196855	0.00053667
BK	25.3422165	0.00019435	0.01107768	0.00291518	0.00079474
Cav3.2	21.952261	0.00032374	0.01812945	0.00294281	0.00080227
Kv1.2	21.7244892	0.00033585	0.01847197	0.00294281	0.00080227
BKbeta1	21.5890293	0.00034333	0.01853969	0.00294281	0.00080227
SK3	19.5539131	0.0004853	0.02572096	0.00363976	0.00099227
Kvbeta2	13.7762737	0.00158793	0.08257252	0.01058622	0.00288603
Cnn1	13.23421	0.00181115	0.09236887	0.01086693	0.00296255
Kir6.1	12.5870915	0.00213155	0.10657732	0.01162662	0.00316966
Kv1.3	12.2040615	0.00235482	0.11538635	0.01177412	0.00320987
Trpp1	11.5218163	0.00282996	0.1358381	0.01306136	0.0035608
Kv4.3	10.6687174	0.00360594	0.16947934	0.01545404	0.0042131
Nos3	9.76977348	0.00473404	0.21776598	0.01790758	0.00488198
Trpc2	9.74206734	0.00477536	0.21776598	0.01790758	0.00488198
Trpv2	8.39938259	0.00745375	0.32796477	0.02630734	0.00717193
Kv3.4	8.15215778	0.00813634	0.34986264	0.02712114	0.00739379
Kvbeta1	7.88136578	0.00897597	0.37699072	0.02834517	0.00772749
SUR2	7.02319241	0.01246042	0.51087703	0.03693151	0.0100683
Kv1.1	6.93146229	0.01292603	0.51704109	0.03693151	0.0100683
Cav1.2	6.61351538	0.01471745	0.57398064	0.04013851	0.0109426
Kv4.1	5.9893527	0.0192319	0.73081201	0.05017016	0.01367744
TASK1	4.7279253	0.03507906	1	0.08769764	0.02390822
Trpc1	4.60135841	0.03745266	1	0.08831916	0.02407766
KChAP	4.55998373	0.03827164	1	0.08831916	0.02407766
Trpm4	3.4096055	0.07343209	1	0.1601327	0.04365553
Kir6.2	3.38111591	0.07472859	1	0.1601327	0.04365553
TWIK1	3.21474314	0.08289243	1	0.17150159	0.04675493
Cav1.1	3.07707214	0.09049527	1	0.1774334	0.04837207
Clca5	3.0570097	0.09167393	1	0.1774334	0.04837207
Kv9.3	2.83338904	0.1061855	1	0.19909782	0.05427824
BKbeta4	2.67937636	0.11784747	1	0.21426813	0.05841399
SK2	2.62001395	0.12276015	1	0.21663557	0.0590594
Kir4.1	2.42602682	0.14066966	1	0.24114799	0.065742
Kv1.6	2.35380507	0.14814732	1	0.24691219	0.06731344
Cav1.3	2.29947901	0.15409464	1	0.24988319	0.0681234
MiRP2	2.23147273	0.16195686	1	0.25572136	0.06971501
Kv3.3	2.11620474	0.17643416	1	0.27143717	0.07399947
Trpc3	1.95648122	0.19919644	1	0.29879467	0.08145769
TASK2	1.49995697	0.28689921	1	0.4198525	0.1144606
KChIP4	1.34342599	0.32717025	1	0.46690215	0.12728732
Trpm3	1.31698978	0.3346132	1	0.46690215	0.12728732
Trpc6	1.2618463	0.35078743	1	0.47662318	0.12993747
Clcn3	1.23993325	0.35746738	1	0.47662318	0.12993747
Kir2.1	1.16011441	0.38308203	1	0.49967222	0.13622113
Trpm2	0.97806233	0.44979873	1	0.56957771	0.15527883
Kvbeta3	0.94547039	0.46308008	1	0.56957771	0.15527883
Trpv4	0.92449004	0.4718602	1	0.56957771	0.15527883
KChIP3	0.9179185	0.47464809	1	0.56957771	0.15527883
Cav3.1	0.70583093	0.57490522	1	0.66447521	0.18114988
Trpm7	0.69805956	0.57897627	1	0.66447521	0.18114988
Kv4.2	0.68299091	0.5869531	1	0.66447521	0.18114988
Kv11.1(erg-1)	0.59965718	0.63306356	1	0.70340395	0.19176267
Trpc4	0.55176836	0.66109264	1	0.70965177	0.19346596
Trpm6	0.54967749	0.66234165	1	0.70965177	0.19346596
SK1	0.34422159	0.79438794	1	0.83619783	0.22796507
SK4(IK1)	0.21508649	0.88322306	1	0.91367902	0.24908806
Trpp2	0.17607811	0.90962499	1	0.92504237	0.25218595
Trpm5	0.14045015	0.93293619	1	0.93293619	0.25433797

## ***Study of the phenotypic switch in mesenteric arteries***

In order to elucidate if the observed changes upon proliferation are specific of the vascular bed studied (femoral artery) or can be extrapolated to other vessels, we have studied the changes in the expression pattern of the ion channels in contractile and proliferative VSMCs from a different vascular bed. We choose mesenteric arteries, as they can constitute a paradigm of a resistance vessel, and we have also studied the expression pattern of the ion channel genes in a model of conduit vessel as it is the case of aortas. Following the same experimental design, we have first explored the relative abundance of the different channel genes in this preparation by using mRNA obtained from the muscular layer of mesenteric and aorta arteries, with endothelium removed as previously described. An overview of the differences in the relative abundance of the channel genes was obtained by a two-way hierarchical clustering analysis of genes and vascular beds (Supplemental Figure IV). The analysis shows that the expression pattern of femoral VSMCs is intermediate between mesenteric and aortic VSMCs. However, there were two groups of genes in which expression in femoral arteries was either lower than in aorta or mesenteric arteries (marked in blue in the figure), or higher than in the other vascular beds (purple frame). Interestingly, the first of these groups includes Kv1.3 and Kv $\beta$ 2 genes, and the second one includes IK1 (SK4). As the up-regulation of IK1 and its functional contribution to proliferation both *in vivo* and *in vitro* has been described in resistance (coronary<sup>11</sup>) and aortic vessels<sup>12</sup>, where no mRNA expression was detected in contractile VSMCs, it is tempting to speculate that not only the expression profile of ion channels but also the changes induced upon PM could be vascular-bed specific.

When analyzing individual gene differences between contractile and proliferating VSMCs from mesenteric arteries, we found that changes in expression were similar to those observed in femoral arteries, although none of the changes towards an increased expression were significant. Nevertheless, the expression profile of ion channels in cultured VSMCs in both vascular beds showed a remarkable similarity (Supplemental Figure V). As shown in the figure, Kv1.3 represents the main Kv1 mRNA present in both preparations. Other similarities are also apparent in other channel families that can deserve a more detail study, as some of them have not been previously reported. One is the presence of BK $\beta$ 4 as the most abundant accessory subunit of BK channels in cultured cells (as opposed to contractile cells, that show a clear predominance of BK $\beta$ 1, see figure 1). Another one is the dominant expression of Kir2.1 among all the Kir channels in cultured cells, while in contractile cells the mRNA expression levels of Kir6.1 and Kir2.2 are about 3 to 5 times higher than those of Kir2.1 (see figure 1). Finally, proliferation in both preparations led to a down-regulation of L-type Ca<sup>2+</sup> channels (mainly Cav1.2) so that mRNA encoding for a T-type Ca<sup>2+</sup> channel (Cav3.1) becomes predominant in cultured VSMCs.

The effects of Kv channel blockers on proliferation (measured as the % of cells incorporating BrdU) were also explored in cultured mesenteric VSMCs (Supplemental figure VIA). In agreement with our results with femoral VSMCs, we found that proliferation rate decreased in the presence of Kv1.3 selective blockers (10 nM PAP-1) being unaffected by blockers of Kv2 channels (50 nM ScTx).

## ***Study of the effects of Kv1.3 blockade on proliferation of cultured VSMCs from human uterine artery***

In a previous work of our group, we have characterized the changes in the expression and function of Kv channels upon phenotypic switch in VSMCs from human uterine arteries<sup>7</sup>, and we found that Kv3.4 channels were up-regulated in cultured uterine VSMCs and their blockade reduced proliferation rate. However, we also described in that work the up-regulation of Kv1.3 channel protein in proliferating VSMCs, so we explored here its possible involvement in uterine VSMCs proliferation. We found that proliferation of human uterine VSMCs is significantly reduced after Kv1.3 blockade (figure VIB), although the absolute magnitude of the effect is smaller than in cultured femoral VSMCs (compare with figure 6D). Altogether, these results suggest that the association between up-regulation of Kv1.3 channels and proliferation of VSMCs may be present in different species and different vascular beds.

## **FIGURE LEGENDS**

**Supplemental Figure I.** Changes in the expression of eNos (as endothelium marker) and Cnn1 (as smooth muscle marker) genes in femoral arteries treated mechanically (with a pipette tip) or/and chemically (by perfusion with 0.1% Triton X-100) to remove endothelial cells. Differences in expression were calculated using Gapdh as endogenous control and clean arteries with intact endothelium as the calibrator. The changes are represented as  $\log(2^{-\Delta\Delta Ct})$ , where

$$\Delta\Delta Ct = \Delta Ct_{problem} - \Delta Ct_{calibrator}$$

and  $2^{-\Delta\Delta Ct}$  represents the expression fold change. Each bar is the mean of 4-6 data from 2 assays for each condition. \* $p < 0.05$ ; \*\*\* $p < 0.001$ .

**Supplemental Figure II. A.** Representative figures of the immunocytochemistry with anti-calponin antibody in cultured femoral VSMCs and HEK cells (used as negative control). Staining of VSMCs was evident even in control media, in the presence of 5% FBS. The lower plots show the quantification of Calponin mRNA (Cnn1) by real time PCR in both preparations. Cnn1 mRNA levels were normalized to the mRNA levels of a housekeeping gene (Gapdh) and Cnn1 levels in contractile femoral VSMCs (tissue) were used as calibrator. We observed a ten-fold decrease in the expression levels of this marker of contractile VSMCs in cultured VSMCs, but there was almost no expression in HEK cells (mRNA levels decreased by  $10^5$ ). **B.** Expression of another two smooth-muscle specific contractile proteins, smooth muscle alpha actin (SM $\alpha$ A) and SM22, was also explored in cultured femoral VSMCs and HEK cells. While SM22 labelling gave a strong signal even in cells cultured in 5% FBS, expression of SM $\alpha$ A was weak in these conditions, increasing dramatically after culturing the cells during several days in the absence of FBS. The figure show the typical labelling detected before (d0) and after 6 days in SF medium (d6).

**Supplemental Figure III.** Changes in the expression pattern of ion channels under proliferation. Differences in expression in cultured VSMCs (red bars) and in the endoluminal lesion at different times (white-grey-black bars) were calculated using the contractile VSMCs expression levels as calibrator. The changes are represented as  $\log(2^{-\Delta\Delta Ct})$ , where

$$\Delta\Delta Ct = \Delta Ct_{proliferative} - \Delta Ct_{contractile}$$

and  $2^{-\Delta\Delta Ct}$  represents the expression fold change. Each bar is the mean of 6-10 data from 3-5 assays in duplicate for each condition. \* $p < 0.05$ ; \*\* $p < 0.01$ ; \*\*\* $p < 0.001$ . Red asterisks indicate p level for cultured VSMCs and black asterisk the p value for the anova test of the endoluminal lesion samples.

**Supplemental Figure IV.** Two way hierarchical agglomerative clustering applied to 59 genes (horizontally) and to samples of VSMCs obtained from mesenteric (M1-M4), femoral (F1-F3) and aorta (A1-A5) arteries (vertically). The input data was the  $\Delta Ct$  value for each gene in each sample, representing the mean of duplicate determinations. Each colour patch in the map represents the gene expression level for each gene and sample. The genes expression levels were normalized within each sample, with a scale ranging from bright green (lowest) to bright red (highest). Missing values are shown as grey patches. The length of the tree branches is proportional to the correlation of the genes expression pattern. Some of these clusters of genes with their correlation coefficients are marked with the yellow boxes that selected (from top to bottom) the genes that are more abundant in conduit arteries (femoral and aorta) than in resistance arteries (mesenteric), the genes more abundant in mesenteric and femoral arteries as compared to aorta and the genes more abundant in resistance vessels (mesenteric). The blue box selected a group of genes showing lower levels of expression in femoral arteries than in the other two vascular beds, that includes the two pore domain channel TWIK and Kv1.3 and Kv $\beta$ 2 subunits. Conversely, the purple box indicates the genes with higher mRNA expression in femoral arteries, including Trpm3, Cav3.a and IK1.

**Supplemental Figure V.** Relative abundance of the ion channel genes studied in cultured VSMCs from mesenteric and femoral arteries. Expression levels are normalized with respect to RP18S and relative abundance was expressed as  $2^{-\Delta Ct}$ , where

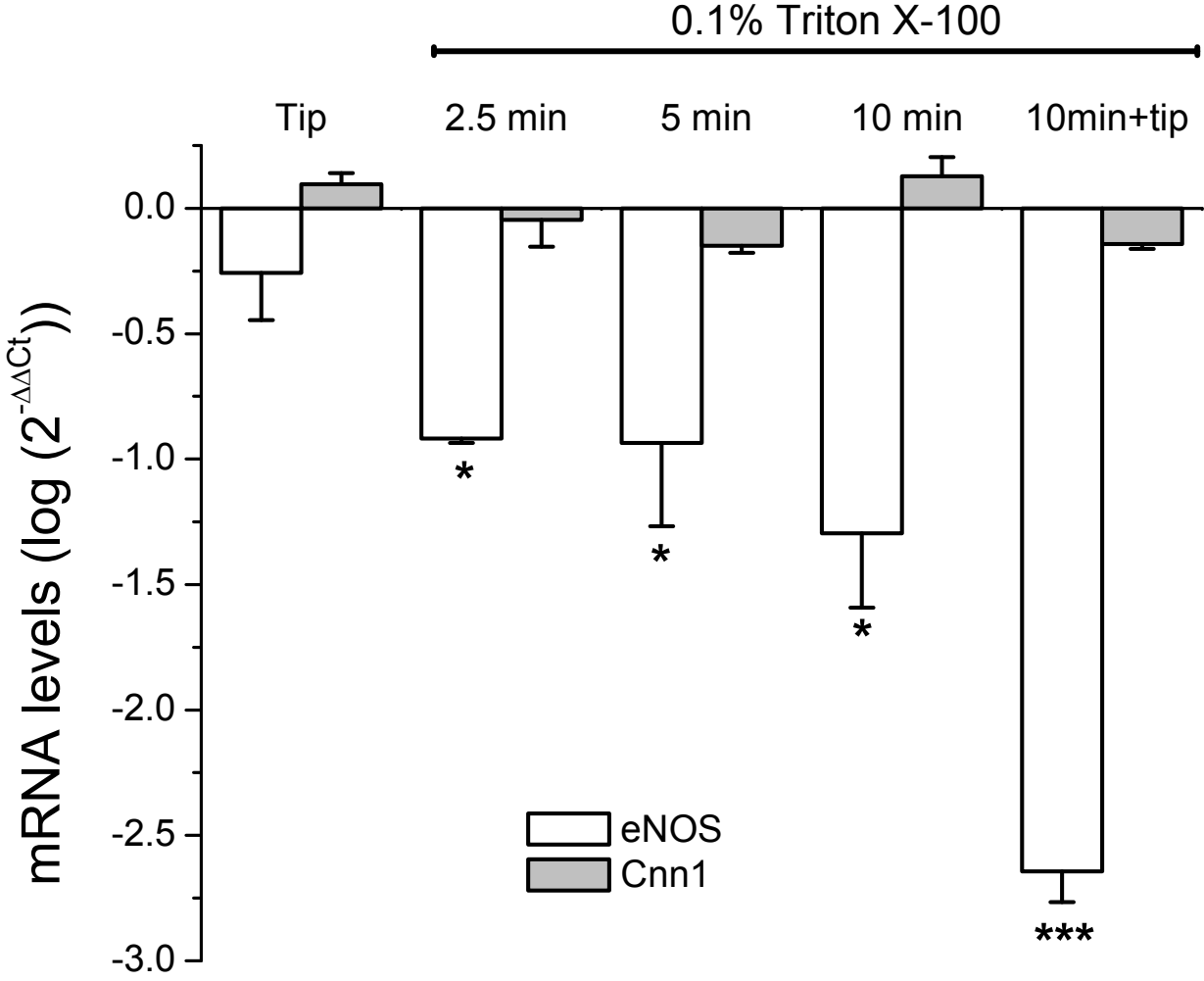
$$\Delta Ct = Ct_{channel} - Ct_{18s}$$

Each bar is the mean of 4-6 determinations obtained in 2-3 duplicate assays. The colour code has been used to identify different gene families.

**Supplemental Figure VI. A.** Study of the proliferation rate (measured as % of cells incorporating BrdU) of cultured mesenteric VSMCs in the absence of FBS (SF, serum-free), or in culture media supplemented with 5% SFB alone (control) or in the presence of a Kv1.3 blocker (10 nM PAP-1) or a Kv2 blocker (50 nM Stromatoxin). \*\*  $p < 0.01$ . **B.** Effect of Kv1.3 channel blockers (10 nM PAP-1 or 10 nM Margatoxin) on proliferation of cultured human uterine VSMCs. Data are mean  $\pm$  SEM of 6 experiments. \*\*  $p < 0.01$ . **C.** Representative images of DAPI staining and BrdU labelling in control and 10 nM MgTx-treated human uterine cultured VSMCs.

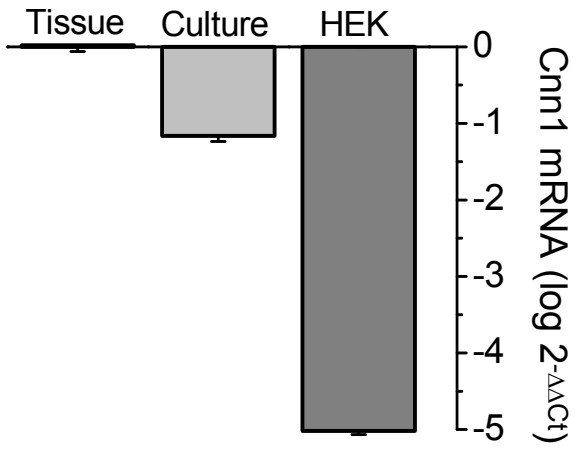
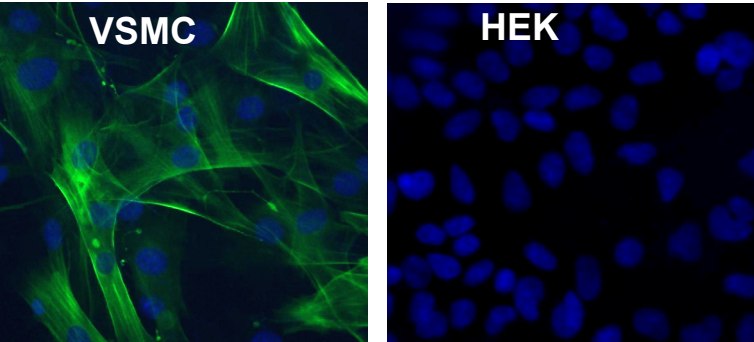
## REFERENCES

1. Roque M, Fallon JT, Badimon JJ, Zhang WX, Taubman MB, Reis ED. Mouse model of femoral artery denudation injury associated with the rapid accumulation of adhesion molecules on the luminal surface and recruitment of neutrophils. *Arterioscler Thromb Vasc Biol.* 2000;20:335-342.
2. Ray JL, Leach R, Herbert JM, Benson M. Isolation of vascular smooth muscle cells from a single murine aorta. *Methods Cell Sci.* 2001;23:185-188.
3. Moreno-Dominguez A, Ciudad P, Miguel-Velado E, López-López JR, Perez-Garcia MT. De novo expression of Kv6.3 contributes to changes in vascular smooth muscle cell excitability in a hypertensive mice strain. *J Physiol.* 2009;587:625-640.
4. Livak KJ, Schmittgen TD. Analysis of relative gene expression data using real-time quantitative PCR and the  $2^{-\Delta\Delta Ct}$  Method. *Methods.* 2001;25:402-408.
5. Eisen MB, Spellman PT, Brown PO, Botstein D. Cluster analysis and display of genome-wide expression patterns. *Proc Natl Acad Sci USA.* 1998;95:14863-14868.
6. Gusnanto A, Calza S, Pawitan Y. Identification of differentially expressed genes and false discovery rate in microarray studies. *Curr Opin Lipidol.* 2007;18:187-193.
7. Miguel-Velado E, Moreno-Dominguez A, Colinas O, Ciudad P, Heras M, Perez-Garcia MT, López-López JR. Contribution of Kv Channels to Phenotypic Remodeling of Human Uterine Artery Smooth Muscle Cells. *Circ Res.* 2005;97:1280-1287.
8. Grifoni SC, Jernigan NL, Hamilton G, Drummond HA. ASIC proteins regulate smooth muscle cell migration. *Microvascular Research.* 2008;75:202-210.
9. Reiner A, Yekutieli D, Benjamini Y. Identifying differentially expressed genes using false discovery rate controlling procedures. *Bioinformatics.* 2003;19:368-375.
10. Storey JD, Tibshirani R. Statistical significance for genomewide studies. *Proc Natl Acad Sci USA.* 2003;100:9440-9445.
11. Tharp DL, Wamhoff BR, Wulff H, Raman G, Cheong A, Bowles DK. Local delivery of the KCa3.1 blocker, TRAM-34, prevents acute angioplasty-induced coronary smooth muscle phenotypic modulation and limits stenosis. *Arterioscler Thromb Vasc Biol.* 2008;28:1084-1089.
12. Kohler R, Wulff H, Eichler I, Kneifel M, Neumann D, Knorr A, Grgic I, Kampfe D, Si H, Wibawa J, Real R, Borner K, Brakemeier S, Orzechowski HD, Reusch HP, Paul M, Chandy KG, Hoyer J. Blockade of the Intermediate-Conductance Calcium-Activated Potassium Channel as a New Therapeutic Strategy for Restenosis. *Circulation.* 2003;108:1119-1125.



**A**

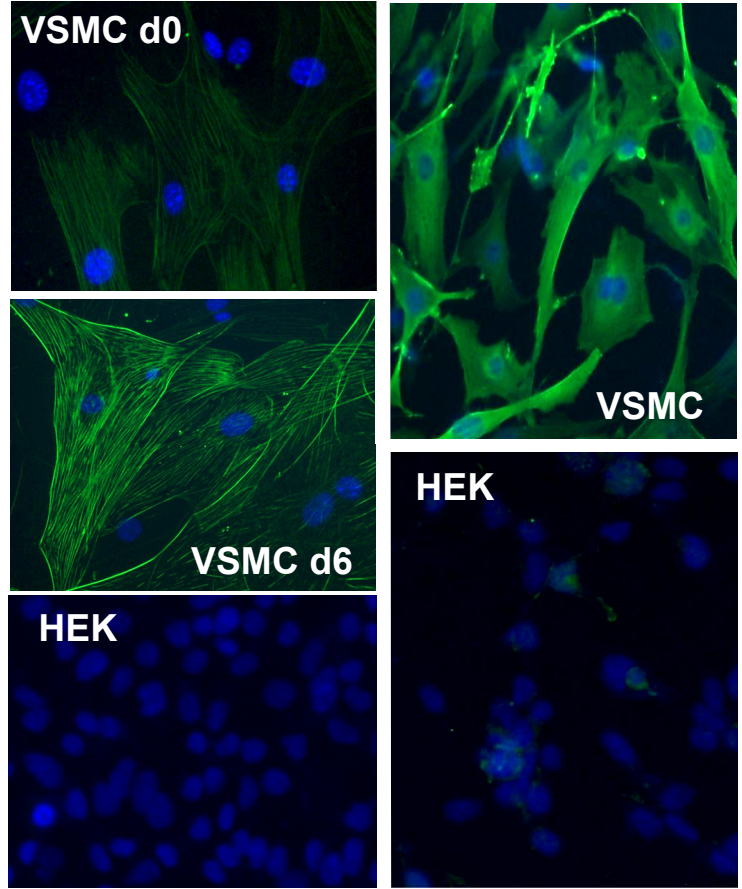
**Calponin**

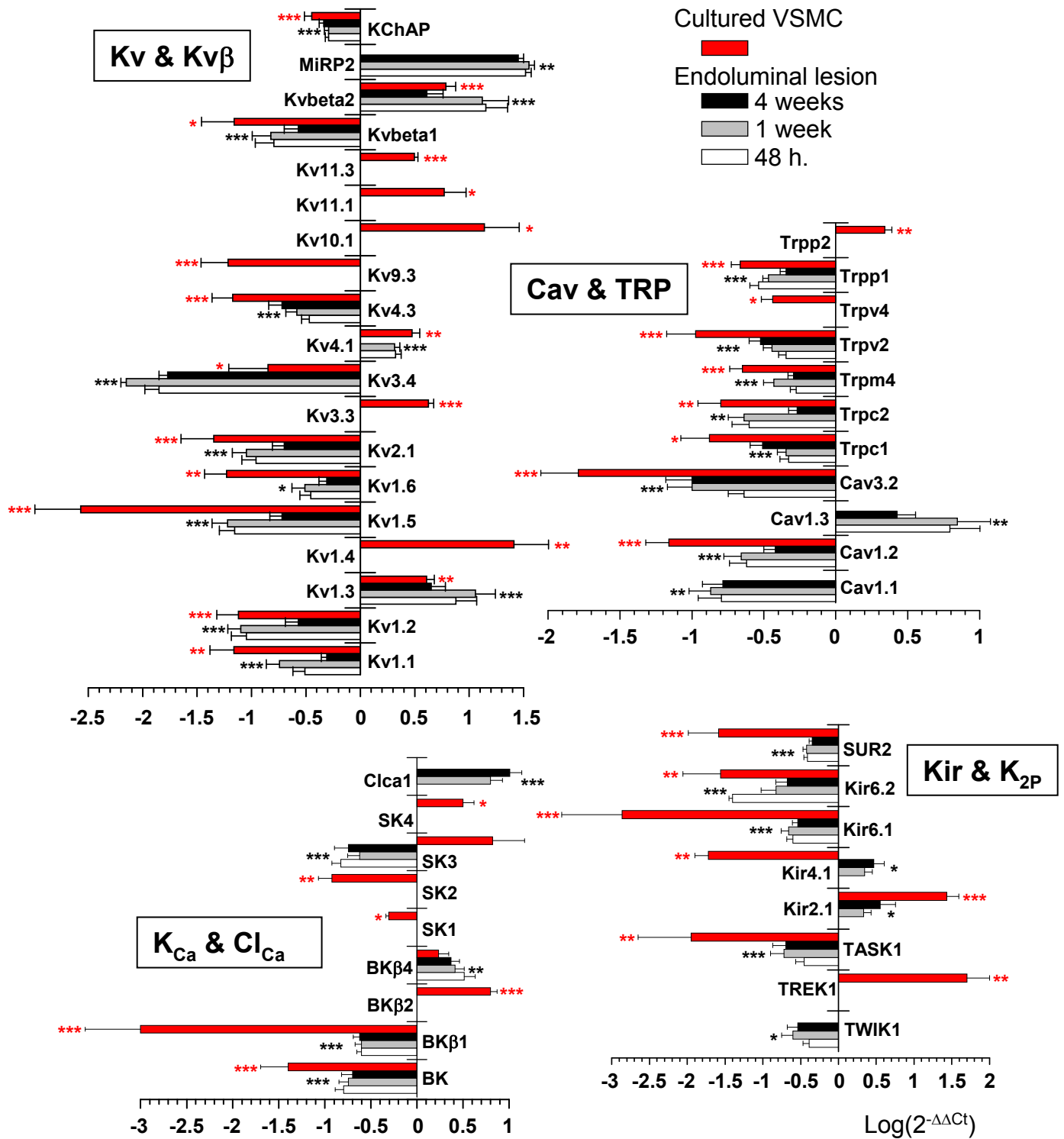


**B**

**SM $\alpha$ A**

**SM22**





Cidad et al., Supplemental Figure IV

